4-20-2010

Synthesis of Fused Heterocyclic Diamidines for the Treatment of Human African Trypanosomiasis and Fluorescence Studies of Selected Diamidines

Jennifer Crystal Brown Barber
Georgia State University

SYNTHESIS OF FUSED HETEROCYCLIC DIAMIDINES FOR THE TREATMENT OF HUMAN AFRICAN TRYPANOSOMIASIS AND FLUORESCENCE STUDIES OF SELECTED DIAMIDINES

by

JENNIFER CRYSTAL BROWN BARBER

Under the Direction of David W. Boykin, Ph.D.

ABSTRACT

A class of linear diamidines was synthesized for the evaluation as a treatment of Human African Trypanosomiasis. These fused heterocyclic compounds are thiazole[5,4-d]thiazoles and are of interest because the parent compound, 2,5-Bis(4-amidinophenyl)-thiazolo[5,4-*d*]thiazole HCl salt, which is also called DB 1929, has exhibited a low nanomolar IC_{50} value against *Trypanosoma brucei rhodesiense* and has shown selectivity for binding to the human telomere

G-quadruplex over that of DNA duplex. A fluoro and a methoxy derivative have been synthesized and are currently undergoing testing for activity and binding affinity. In addition, fluorescence studies of selected diamidines were done to study the effect of structural variation on fluorescence. This data is useful since it can determine what types of moieties are needed to yield a compound that will fluoresce in the higher wavelengths (500 nm and above) of the visible spectrum, which would be advantageous in determining the uptake of the drug in the trypanosome within the endemic areas of Africa with a simple microscope.

INDEX WORDS: Organic synthesis, Heterocyclic chemistry, Human African Trypanosomiasis, Sleeping sickness, Fused heterocycles, Linear diamidines, UV-Visible spectroscopy, Fluorescence spectroscopy, *Trypanosoma brucei gambiense*, *Trypanosoma brucei rhodesiense*

SYNTHESIS OF FUSED HETEROCYCLIC DIAMIDINES FOR THE TREATMENT OF HUMAN AFRICAN TRYPANOSOMIASIS AND FLUORESCENCE STUDIES OF SELECTED DIAMIDINES

by

JENNIFER CRYSTAL BROWN BARBER

A Dissertation Submitted in Partial Fulfillment of the Requirements for the Degree of

Doctor of Philosophy

in the College of Arts and Sciences

Georgia State University

2010

SYNTHESIS OF FUSED HETEROCYCLIC DIAMIDINES FOR THE TREATMENT OF HUMAN AFRICAN TRYPANOSOMIASIS AND FLUORESCENCE STUDIES OF SELECTED DIAMIDINES

by

JENNIFER CRYSTAL BROWN BARBER

Committee Chair: Dr. David W. Boykin

Committee: Dr. Alfons Baumstark

Dr. W. David Wilson

Electronic Version Approved:

Office of Graduate Studies

College of Arts and Sciences

Georgia State University

May 2010

DEDICATION

The completion of my dissertation is dedicated to the amazing people that have helped me get through this trying time. First I would like to thank my mother, Evelyn Boney. If it were not for her there would be no me. She struggled her entire life such that I could have everything that I needed including food, clothes, a home, and most importantly, a proper education. Your love of reading made me enjoy reading. This love of reading fed my desire for knowledge and that desire for knowledge has gotten me to this point. I know that I will never be able to completely repay you for all that you have done for me. Know that I will never stop trying. I will always love you.

Secondly, I would like to thank Roger Clements for being like a father to me for the last 15 years. I am not your birth child but I have never felt any less. Thank you for always being there for me. You almost sacrificed yourself to keep a promise to me and I will never forget that. I will always love you.

I would also like to thank my wonderful husband, Jamaal Barber. We have known each other for over 11 years and you have always supported my educational aspirations. Many other prospective suitors were intimidated by my dreams of being a scientist. Thanks for making me feel like the smartest, most beautiful woman in the world everyday. Thanks for giving me those pep talks before tests and presentations. Thanks for loving me and for giving me the best gift ever, our daughter, Sydney Barber. I love you more than you will ever know.

My daughter Sydney is the next person on my thank you list. You are too young to realize it but it is you that has given me the renewed desire for the pursuit of my dreams. I work hard everyday to provide for you. I hope that I am able to be as great a role model for you as

your grandmother has been for me. Remember to never give up on your dreams. You will face many obstacles but none of them are insurmountable. I love you more than you will ever know.

In addition, I would like to thank some angels that have had an impact in my life. Gladys Brown was a loving grandmother that was not able to see this day but I know she is proud of me. Avery Williams was a great friend that departed this world way before what should have been his time and Jasmine Peters was a loving little girl that will always hold a special place in my heart. I love and miss you all dearly.

Last but not least I would like to thank that higher power. My journey to this point was not smooth or easy but it has definitely been an adventure. Even during my bad experiences I was able to meet some great people and learn some valuable lessons. Thanks for always providing for me and giving me the courage and strength to endure. Thanks for always putting the right people in my life at the right time.

ACKNOWLEDGMENTS

There are numerous people that have helped me get to this point in my career. I would first like to thank my advisor, David Boykin. You are the greatest boss that a graduate student could ask for. You were always willing to share your vast knowledge and your passion for science is infectious. Thank you for everything.

I would also like to thank our departmental collaborator David Wilson. Thanks for allowing me to continue my studies in your lab during my pregnancy. I understand so much more about my work because of my time spent in your lab.

Thank you to my group members: Chad, Bin, Laixing, Arvind, Alpa, Cardra, Rafay, Timmeda, Paul, Kate, Mohamed, Reem, Danuta,, Martial Say, Mariusz, Liu, Abdelbasset, and Maloy. You have all helped to make me a better scientist.

Thank you to the Wilson groups members as well: Farial, Catherine, Denise, Ha, Marium, Rupesh, Yang, Manoj, Kedar, Rebecca, Jessica, and Joe. Thanks for being so willing to help me acclimate to your lab.

Several friends have also helped me to get to this point. LaToya has always been my connection to home, Nicole helped me get through my undergraduate studies at East Carolina University, LaKeisha and Ejae got me started on this journey called graduate school at Georgia Institute of Technology, Amy, Charmita, Gurpreet, Janet, Sandra, Suazette, and Julianne have been there to help me complete it at Georgia State University. You guys are more important to me than you will ever know. The knowledge that you all have given me has not only allowed me to become a better scientist but a better woman, friend, wife and mother.

There are many more people that have been a part of this journey but were not mentioned. They include my all of my teachers from elementary school and beyond, program coordinators, friends, family, and numerous others. You too have been instrumental in getting me to this point. I owe you much gratitude.

TABLE OF CONTENTS

LIST OF FIGURES

LIST OF SCHEMES

LIST OF TABLES

LIST OF EQUATIONS

LIST OF ABBREVIATIONS

δ	Chemical Shift
λ	Wavelength
π	Pi
$\Delta\bar{\upsilon}$	Change in wavelength (in wavenumbers)
$\bar{\upsilon}_a$	Absorption maximum
$\bar{\upsilon}_f$	Emission maximum
au	Arbitrary units
DB	Dave Boykin
DCM	Dichloromethane
DMF	Dimethylformamide
DMSO	Dimethylsulfoxide
DNA	Deoxyribonucleic acid
EtOH	Ethanol
FDA	Federal Drug Administration
h	Hours or Plank's constant
HCl	Hydrochloric acid
H_2O	Water
IR	Infrared
max	Maximum

MeOH	Methanol
min	Minute
ml	Milliliter
N	Nitrogen
Na_2CO_3	Sodium Carbonate
NaOH	Sodium Hydroxide
nm	Nanometer
ns	Nanosecond
O	Oxygen
o	Ortho
p	Para
pH	Potentional for hydrogen ion concentration
ppm	parts per million
RNA	Ribonucleic acid
S	Sulfur
s	Second
s^{-1}	1/Second
Se	Selenium
S_n	Singlet state, n = 0, 1, 2, 3, etc.
Te	Tellurium
THF	Tetrahydrofuran
TLC	Thin layer chromatography
T_n	Triplet state, n = 0, 1, 2, 3, etc.

1. AFRICAN TRYPANOSOMIASIS

1.1. History of the Disease

Protozoa are eukaryotic, unicellular organisms that can infect both vertebrates and invertebrates. There are more than 66,000 species and about 10,000 of the living ones are parasitic. These organisms are unusual in that they have the ability to replicate within the host to create hundreds of thousands of themselves in a short time frame.[1]

Protozoa consist of a membrane, surface coats, and a cytoplasm, within which many of the common subcellular organelles are found. They digest particulate matter by liposomal enzymes and excrete waste by either diffusion or phagocytosis. They can be mobile and use both the sexual and asexual forms of reproduction.[1]

Human African trypanosomiasis is a parasitic, protozoan disease that exists in two hemoflagellate forms, *Trypanosoma brucei (T. b.) gambiense* and *T. b. rhodesiense*. These organisms are transmitted through the bite of the tsetse fly. The tsetse fly is in the genus of *Glossina (G)* and is endemic to countries in Africa near the equator.[1] Over 60 million people are at risk of getting infected with human African Trypanosomiasis and it is always fatal if left untreated.[2] An epidemic exists in four countries, namely Uganda, Sudan, Angola, and the Democratic Republic of the Congo. Some areas have over 20% of the population infected with the disease.[3]

Human African trypanosomiasis is also known as sleeping sickness and has been known since at least 1742. A cattle disease called nagana was attributed to the tsetse fly transmission of the trypanosome in 1895. The disease is now referred to as cattle trypanosomiasis and has hindered the economic growth of an entire section of tropical Africa due to difficulties with cattle ranching. Cattle trypanosomiasis is caused by *T. b. brucei* but it does not infect humans.[2]

T. b. gambiense is the human equivalent of this disease. Forde first discussed it in 1902 literature and its counterpart, *T. b. rhodesiense*, was described eight years later in 1910 by Stephens and Fantham. In 1912, Kinghorn and Yourke used experimentation to prove that the *rhodesiense* form of the disease was capable of being transmitted from humans to animals by the tsetse fly. They also reached the conclusion that game animals such as the impala and warthog were cable of serving as reservoir hosts for the East African form of the disease.[1]

1.2. Trypanosoma brucei gambiense

T. b. gambiense is also called West African or Gambian trypanosomiasis.[4] It is generally found in western and central Africa, including Ivory Coast, Senegambia, Liberia, Guinea, Ghana, Benin, Cameroon, Nigeria, Gabon, Zaire, and Uganda.[1] *T. b. gambiense* is caused by the 'riverine' tsetse flies *Glossina palpalis*, *G. tachinoides*, and *G. fuscipes*. The natural habitat of these flies lie near rivers and forests that have dense foliage. Humans are the preferred food source but they will prey on whatever food sources are available at the time, including pigs, dogs, and goats.[4] *T. b. gambiense* has an incubation period that is several weeks to months but it can be months to years before the brain is affected after infection.[1] As a result, it is referred to as the chronic form of the disease.[2] Most hosts are symptom-free during the long incubation period. This enables the parasite to adapt to the host and contributes to the spread of the disease.[4]

1.3. Trypanosoma brucei rhodesiense

T. b. rhodesiense is also called East African or Rhodesian trypanosomiasis.[4] It is limited to East Africa, namely Zimbabwe, Zambia, Tanzania, Uganda, and Kenya.[1] *T. b. rhodesiense* is transmitted by *G. morsitans*, *G. pallidipes*, and *G. swynnertoni*. The natural

habitats of these flies are the lakes and savannah of the region. These flies are more particular about their food source with antelope and cattle being the primary sources. Many other animals can become infected but are not good hosts since they either perish quickly or the disease has a short life span. *T. b. rhodesiense* is unique in that it is a zoonosis, or a disease that is capable of being transmitted from vertebrate animals to humans.[4] *T. b. rhodesiense* has an incubation period of 2-3 weeks and generally runs its course in several weeks with the brain being affected 3-4 weeks after infection.[1] As a result, it is referred to as the acute form of the disease.[2]

1.4. Life Cycle of the Fly

The genus *Glossina* has over 20 species of the tsetse fly that are all localized in Africa.[4] Only six species of *Glossina* serve as vectors for the human form of the disease and it can be transmitted by both sexes of the fly. The infective stage is also called the metacyclic or metatrypanosome stage. It occurs when the tsetse fly injects the parasites that lie in the salivary glands through its bite. The trypanosomes then migrate to the blood of the host and begin to divide by binary fission at the infection location. This causes a chancre sore to form at the site of the bite. The lymphatic system is used as the access mode to the bloodstream and further divisions can occur there.[1]

The tsetse fly becomes infected when it takes a blood meal from an infected host. The parasite reaches the gut of the fly and become procyclic trypomastigotes. They divide for another 10 days and eventually migrate to the salivary glands. Once they reach this location, they become epimastigotes, which then further divide and become metatrypanosomes. This form of the parasite is actually the infective agent. The cycle of migration and division varies for each species of the *Glossina* fly but generally lasts anywhere from 25 to 50 days. The strain of the

trypanosome and the local temperature are also variables that affect the length of the life cycle of the fly.[1]

The fly is now infected for life and can infect the host with more than 40,000 metatrypanosomes per bite. It should be noted that the minimum dose for infection of a host is only 300-500 metatrypanosomes. Another possible source of infection occurs with the ingestion of raw meat from an infected animal.[1]

1.5. Pathogenesis of the Disease

The trypanosome is unique in that it has two mechanisms for preventing the host from eliminating it. The first such mechanism involves the ability to vary its surface antigens. After a host has been infected, its initial response is to produce antibodies against the trypanosome surface antigens. These surface antigens are glycoproteins that coat the trypanosome. The antibodies are produced but a few trypanosomes have a protein coat that is slightly different, allowing them to avoid elimination. These few trypanosomes are replicated and the new antigenic variation attacks the host. The host initiates a second response by producing another set of antibodies that are more specific for this second antigenic variation. Again the majority of the population is destroyed but a few survive. This cycle continues until the newest antigenic variant is capable of defeating the host.[1]

The second mechanism involves immune suppression. When the parasite is introduced, B-lymphocytes and macrophages are nonspecifically stimulated. The cells are then able to multiply and their response to antigens is increased. On the other hand, the host's T-cell dependent immune responses to the antigens are depressed. This is due to the ability of the parasite to arouse the host's immune response nonspecifically such that the response is not specifically towards the trypanosome.[1]

1.6. Clinical Diagnosis

The disease is generally the same for the two types of trypanosomes being discussed with the only difference being the time scale for the infection. A chancre at the site of the bite from the fly is the first sign of infection. The lesion generally appears at 5-15 days after the infection and the parasites are localized at that site for the interim.[1, 4] The lesion will spontaneously diminish after 2-3 weeks. Once the incubation period is over, the parasites move to the bloodstream of the host. This occurs from a few hours to days after the initial emergence of the chancre. If no chancre ever presents itself, then the migration to the bloodstream will occur 1-3 weeks after infection.[4] At this point in the infection period, numerous symptoms are possible. They generally lack a pattern and are inconsistent. The symptoms can even vary within the same type of sleeping sickness. Some of the more common symptoms include fever, rash, enlarged lymph nodes, enlarged and softened spleen, jaundice, eye disease, and cardiovascular and endocrine system crisis. The final phase of the disease is the movement of the parasites to the central nervous system (CNS). The disease can progress to this stage in weeks to months for the Rhodesian form or months to years for the Gambian form. The symptoms at this stage include headache, stiff neck, and personality and behavior changes, to name a few. Eventually, mental deterioration, seizures, speech impediments, tremors and narcolepsy may occur. The final symptoms include the inability to arouse the patient, dribbling of saliva, and wasting, or the taking away of strength and energy. These symptoms eventually lead to the occurrence of a coma and the patient will usually pass away without regaining consciousness.[1, 4] The Rhodesian form of the disease can be so swift such that death may occur prior to the CNS symptoms occurring.[4]

1.7. Medication History

1.7.1. Arsenicals

Sleeping sickness was first treated with compounds that contained arsenic. The first was called atoxyl (**1**). Thomas and Beirne first discovered the trypanocidal activity of atoxyl in 1905. It was used to treat about 90,000 patients in Cameroon and the Congo in the early 1920's. Atoxyl did provided some improvement of the disease symptoms but it was rarely able to cure the disease and frequently led to the severe side effects of optical atrophy and blindness. A second arsenical, tryparsamide (**2**), was synthesized in 1922 by Jacobs and Heidelberger. This drug was better than atoxyl in that it was able to cure at least 50% of the patients that took it. The negative was that it still caused the severe side effects of optical atrophy and blindness in 5% of patients. Tryparsamide and suramin (**3**), which will be discussed later, were used in combination in the 1930's for over 300,000 patients. In 1938, Friedheim discovered melarsen (**4**) and in 1946 he discovered melarsoprol (**5**). Melarsoprol is also called Mel B and was less toxic than tryparsamide.[5-8]

The trivalent aromatic arsenicals (As^{+3}) are very active against trypanosomes in vitro but are highly toxic in vivo. Pentavalent aromatic arsenicals (As^{+5}) were less toxic in vivo but lacked trypanocidal activity in vitro, as compared to the trivalent variety. It was found that the pentavalent aromatic arsenicals could be reduced in vivo to the active trivalent form. Atoxyl, tryparsamide, and melarsen are examples of the pentavalent aromatic arsenicals that, upon reduction, form active compounds in vivo. Melarsoprol was created by reacting melarsen oxide (**6**), a toxic trivalent aromatic arsenical, with 2, 3-dimercaptopropanol (**7**), which is also known as British Anti-Lewisite (BAL). The product, melarsoprol, maintained its activity against trypanosomes but was much less toxic.[5, 9, 10]

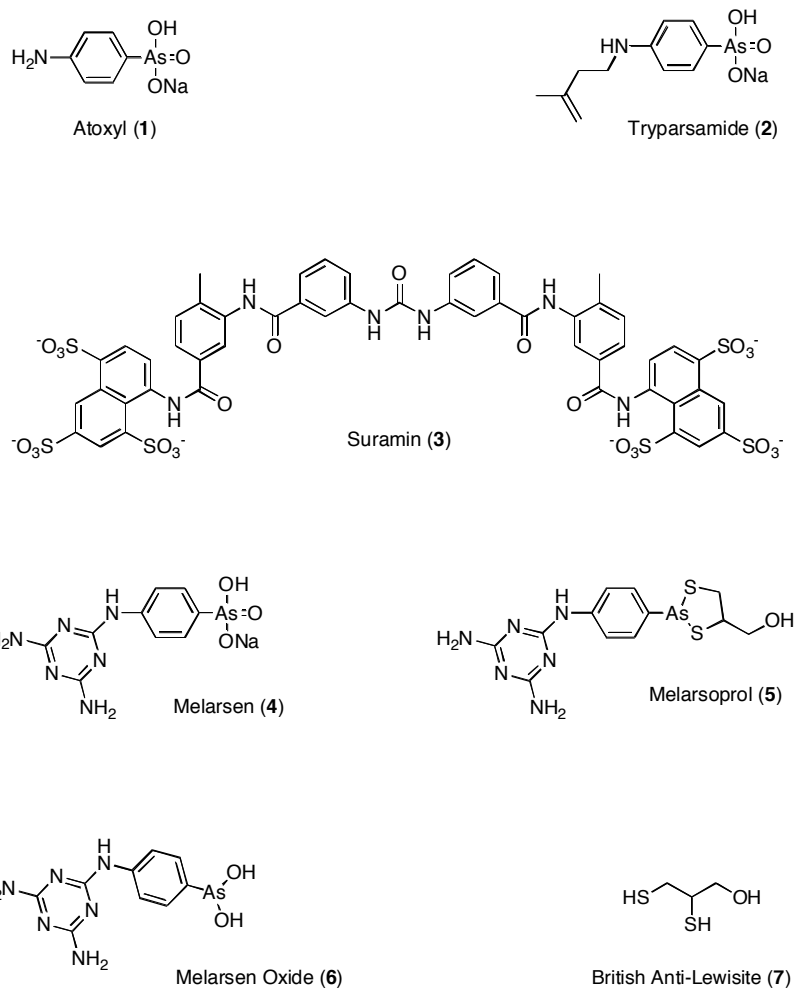

Figure 1 Structures of Atoxyl (1), Tryparsamide (2), Suramin (3), Melarsen (4), Melarsoprol (5), Melarsen Oxide (6), and British Anti-Lewisite (7)

As previously stated, atoxyl and tryparsamide often caused optic atrophy or blindness. The use of melarsoprol did not cause these severe side effects but as much as 18% of treated patients developed encephalopathy, which was sometimes fatal. Patients treated with melarsoprol also developed mild renal issues, nausea, diarrhea, dermatitis, and hypertension.[5]

Arsenicals are generally nonpolar drugs that are able to cross the blood-brain barrier. This property allows arsenicals to be used for the treatment of patients where the disease has

affected the CNS. Melarsoprol is the drug of choice at this stage but prior to administration, confirmation of the disease stage must be characterized using either parasites, elevated protein, or cell numbers in the cerebrospinal fluid (CSF) or by seeing definitive CNS symptoms in the patients.[5]

1.7.2. Melarsoprol

As previously stated, melarsoprol (**5**) is used in the treatment of the late stage of human African trypanosomiasis. It must be administered intravenously and at a slow rate since the drug will cause pain and necrosis at the site of contact. There is no defined course of treatment for the administration of melarsoprol. Some medical professionals prefer to use a maximum daily dosage whereas others tend to gradually increase the dosage over time. Still other medical professionals calculate the dosage based on the patients cardiac risk. Most treatment regimens include an introductory dosage of either suramin (**3**) or pentamidine (**8**), for *T. b. rhodesiense* and *T. b. gambiense* infections, respectively. Following treatment, 80-90% of the patients are cured but some of those that develop the disease again will be resistant to treatment with melarsoprol.[4, 11]

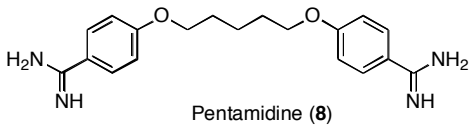

Pentamidine (**8**)

Figure 2 Structure of Pentamidine (8)

Side effects of melarsoprol treatment can occur instantly following the injection. These side effects include malaise, diarrhea, vomiting, and fever. Other side effects that usually do not occur with subsequent injections include rash, tachycardia, and swelling of the lips and tongue. Some of the more severe side effects include paralysis, cardiac arrhythmia or arrest, and

encephalopathy. Encephalopathy occurs with 1-11.4% of melarsoprol treated patients and it can initially present itself in several ways with the final stage being that of a deep coma that may involve convulsions. Once the neurological problems arise, the melarsoprol administration ceases until consciousness is regained. At this point, the drug regime can begin again at lower dosage levels. Unfortunately, 50% of the treated patients will have a fatal response once the disease progresses this far.[4]

1.7.3. Suramin

Ehrlich and his colleagues tested dyes for possible trypanocidal activity. Two of them had weak *in vivo* activity. They were naphthylaminesulfonic acid derivatives called nagana red (**9**) and trypan red (**10**). This lead to the synthesis and testing of other derivatives for trypanocidal activity. One such derivative, suramin (**3**), was found to be effective. Suramin was put into production in 1916 by Bayer. Several derivatives of suramin have been synthesized and tested but none of them compared to suramin with regards to activity.[5, 6, 12]

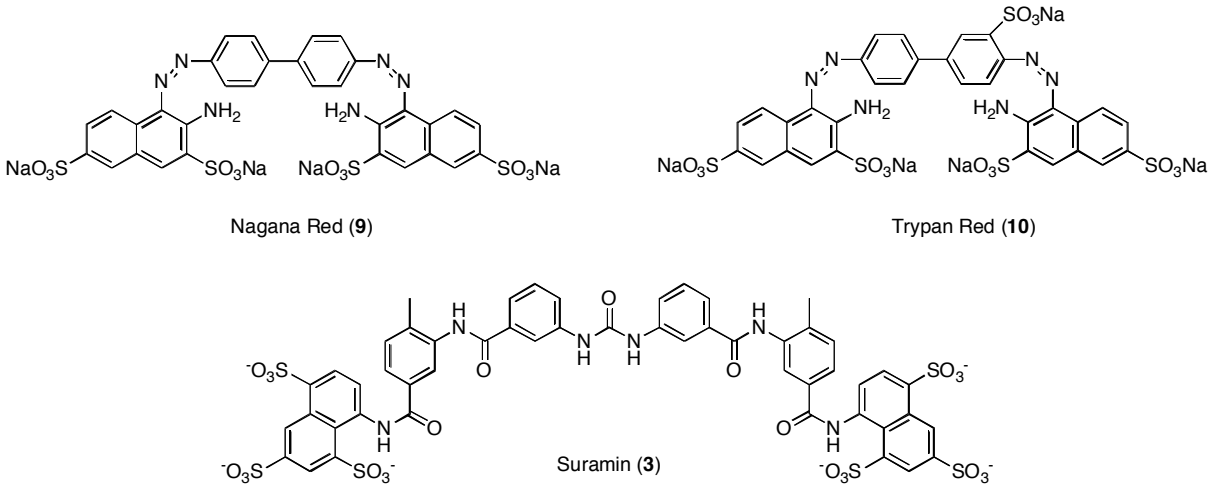

Figure 3 Structures of Nagana Red (9), Trypan Red (10), and Suramin (3)

Some significant discoveries about the mode of action of the drug have been discovered. Hawking saw that trypanosomes would loose motility *in vitro* after a 6 hour incubation period with 4 nM of suramin. Lower concentrations of the drug were effective to some extent against the trypanosomes. This lead to the belief that suramin does not kill the parasites immediately. Instead, is causes subtle biochemical changes that ultimately kill the trypanosome. *In vivo*, it takes up to 24 hours after administration of the drug before the trypanosomes are removed from the bloodstream. It has also been discovered that several enzymes in various organisms are sensitive to suramin. It was found that some trypanosomal enzymes are sensitive to suramin but the mammalian versions are not and that some trypanosomal enzymes that are not found in mammals are also affected by suramin. The sensitivity of these enzymes to suramin contribute to the discerning ability of suramin for trypanosomes.[5]

Suramin must be administered intravenously. The recommended dosage is 20 mg/kg of body weight per injection with the maximum being 1000 mg per injection. A test injection of suramin should be given to the patient to gage the effect of the drug on the patient followed by the regular dosage conditions. Suramin administration generally involves five to seven injections every five to seven days over the course of 21 days with a weekly dosage administered for an additional five weeks.[4]

Treatment with suramin causes many problems within patients. Some of the side effects of treatment include optical atrophy, blindness, renal failure, and rash. Less than 1% of treated patients develop an idiosyncratic reaction that results in vomiting, nausea, seizures, and loss of consciousness.[5]

Suramin is a polar molecule and cannot cross the blood-brain barrier. It is therefore generally used for the initial stage of the disease but it has been used in combination with

melarsoprol (**5**) for the late stage of the disease. It should be noted that the combination therapy did not provide any significant improvement in trypanocidal activity as compared to the use of melarsoprol alone.[5]

1.7.4. Eflornithine

Eflornithine (**11**), or DL-α-difluoromethylornithine (DFMO), was synthesized in the 1980's as a cancer drug. It was too toxic for cancer therapy but had some *in vivo* activity against trypanosomes.[3, 13] Elfornithine is usually used to treat patients that are resistant to melarsoprol (**5**) in the late stage of the disease.[2, 3] Eflornithine has side effects similar to other cancer drugs including anemia, fever, alopecia, vomiting, dizziness, and diarrhea.[3]

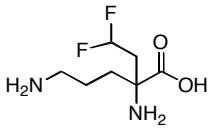

Eflornithine (**11**)

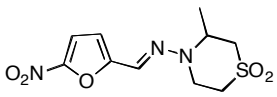

Nifurtimox (**12**)

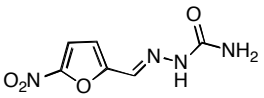

Nitrofurazone (**13**)

Figure 4 Structure of Eflornithine (11), Nifurtimox (12), and Nitrofurazone (13)

1.7.5. Nitrofurans and Nitroimidazoles

Some nitrofurans and nitroimidazoles have *in vivo* trypanocidal activity. Nifurtimox (**12**) is used to treat the acute form of Chagas' disease, or American trypanosomiasis, and it has been found to have some activity against African trypanosomes. Nitrofurazone (**13**) can cross the blood-brain barrier and is used in the late stage treatment of African trypanosomiasis if the patient has resistance to the arsenical drugs. Nitrofurans (nitrofurazone and nitrofurtimox) are highly toxic and can have mutagenic or carcinogenic properties.[5, 14] They are the second choice drug behind melarsoprol (**5**) and eflornithine (**11**) for the last stage of the disease.[2]

1.7.6. Nifurtimox

Nifurtimox (**12**) has activity in both stages of *T. b. gambiense*. Since it has yet to be approved for use in human African trypanosomiasis, it has only been used in patients the are resistant to melarsoprol (**5**). In one trial of 75 patients in the late stage of the disease, 72% were cured using a treatment regimen that consisted of a 15 mg/kg per day dosage for 14 to 45 days. A second trial had 15 patients that used a 4-5 mg/kg dose 3 times a day for 60 days and it yielded an 87% cure rate.[3]

The side effects of the drug are difficult to distinguish since the drug is given to patients in the last stage of the disease that have developed resistance to melarsoprol. Generally, the side effects that the patients were having prior to administration of nifurtimox were exacerbated.[3]

1.7.7. Diamidines

Throughout this dissertation, diamidine structures are shown as a free base, however, when used in biological systems, they are protonated and dicationic.

Synthalin (**14**), or 1, 10-Diamidinodecane, was the first diamidine that was discovered to be effective at killing trypanosomes. It was tested by Jansco and Jansco in 1935 for its suspected ability to prevent the growth of the trypanosome *in vivo* due to hypoglycemia but this was proved to not be the cause of the lack of trypanosome growth. Two years later in 1937, pentamidine (**8**), propamidine (**15**), and stilbamidine (**16**) were tested followed by the testing of berenil (**17**) in 1955.[5, 15-18]

It was initially believed that diamidines interacted with DNA and that this interaction causes the trypanocidal activity. The diamidines were thought to form salt bonds with the phosphate groups of the DNA. These bonds then allowed the diamidines to insert itself into the DNA minor groove near an A-T pair.[5] Diamidines are charged molecules that cannot pass the

blood-brain barrier. The inability to cross the barrier means that they are only effective against the initial stage of the disease.[5]

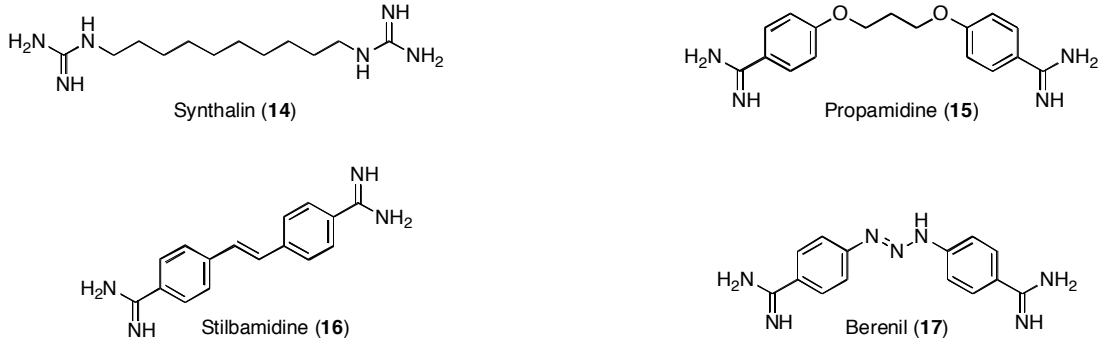

Figure 5 Structure of Synthalin (14), Propamidine (15), Stilbamidine (16), and Berenil (17)

1.7.8. Pentamidine

Pentamidine (**8**) is the more widely used drug of the diamidine class.[5] It is used to treat the early stage of the disease and has an advantage over suramin (**3**) in that it has a shorter time course for drug administration. Pentamidine must be administered intramuscularly and the dosage recommendation is no more than 4 mg/kg of body weight per day with an injection every day or every other day for 7-10 days.[2, 4]

Pentamidine causes nephrotoxicity and hypotensive occurrences in patients. Other side effects include tachycardia, fainting, vomiting, and sometimes hypoglycemia.[5] A common side effect is pain and inflammation of the skin at the injection site. Some of the side effects can be seen instantly following the injection of the drug and are attributed to the rapid decent of the patients blood pressure that occurs when the drug is administered too quickly.[4]

1.7.9. Berenil

Berenil (**17**), or diminazene, is a pentamidine (**8**) analog that was developed to treat trypanosomes in cattle.[2, 3] It has been used in several countries for the human form of the

disease and is listed by the World Health Organization (WHO) as a trypanocidal drug, but berenil has never been registered for human use.[2] During shortages of pentamidine, berenil was used to treat patients in the initial phase for both forms of the disease.[3]

When used to treat humans, berenil is administered intramuscularly at 5-7 mg/kg of body weight in up to 3 injections over 2 days. The rate of patient relapse is 3-15% and it has side effects that resemble pentamidine except that it has a much less painful injection. It also has a shorter course of treatment as compared to pentamidine.[3]

2. THE INTERACTION BETWEEN DNA AND DRUGS

2.1. Medicinal Chemistry

Merriam-Webster's dictionary defines the word medicinal as tending to or used to cure disease or relieve pain and chemistry as the science that deals with the composition, structure and properties of substances and the transformations that they undergo.[19] If the two words are then put together as medicinal chemistry then the definition would be the science of substances that are intended for the treatment or cure of a pain or disease. Furthermore, the substances that are used for the treatment of pain and disease are called medicines and drugs are the constituent parts that the medicines are composed of. Today medicinal chemistry is composed of many divisions, including but not limited to the study of the chemical transformations and excretion of the drug, the isolation of natural products, determination of biological activity, and the synthesis of unique molecules.[20]

Medicinal chemistry dates back thousands of years. It began when people treated their ailments with roots, berries, tree bark, and herbs. Many of these natural materials were successfully employed but were randomly utilized. It was not until the last two centuries that the investigation into what ingredient was the cause of the successfulness of the natural source began. Today if a natural product is found to have some activity towards a disease, its molecular composition will be determined followed by the synthesis of individual fragments, which are tested to determine which component is causing the desired effect.[20] This component is then known as the active or lead compound.[21] The approach used by our early ancestors is considered to be rather random since they lacked the forethought to be certain which natural source would be useful for a specific ailment. The use of this random trial and error method has

evolved into a more rational, or targeted, approach that is referred to as drug discovery and design.[20, 21]

2.2. Drug Discovery and Design

In drug discovery, the lead compound that was isolated from a natural product may be synthetically altered to intensify the desired properties and to diminish the negative properties. Once these modifications are complete, the compound is referred to as a drug candidate and will undergo several studies, including, but not limited to, biological, animal, and pharmacological studies. Once satisfactory testing results are received, the compound is a clinical candidate and can be moved into clinical trials. If the candidate drug yields adequate clinical trial data, then it can be marketed to the public following FDA approval.[20]

Since the random discovery of successful drugs is few and far between, pharmaceutical researchers use a more rational approach in the quest for new drug entities. This rational approach involves finding a molecular target for a disease of interest followed by designing a compound that will ultimately interact with that target. The target will generally be a receptor, enzyme, or nucleic acid. A receptor consists of a protein that is set into the walls of the cell membrane such that a portion of it rests outside the actual cell. The surface of the protein has an irregular shape but a part of it is an exact match for a specific molecular messenger. This part of the receptor is called the binding site since the messenger will fit perfectly in the site. The fitting of the messenger into the binding site of the receptor causes the receptor to be activated and a message to be transmitted from the messenger to the cell.[21]

An enzyme is a catalyst used to speed up the rates of biological reactions that take place in a cell. Enzymes are specific to their function and to the metabolic reaction that they act on. This specificity causes a substrate to be converted into a precise product. Enzymes are generally

significantly bigger than its corresponding substrate and a small segment of it is referred to as the active site. The active site is the part of the enzyme that has a structure that is complementary to a particular part of the substrate. The complimentarity of the structure between the two species enable them to identify each other and bind using weak forces such as ionic bonds, hydrogen bonds, or van der Waals interactions. The binding of the enzyme to the substrate thereby results in the acceleration of the metabolic reaction.[22]

Nucleic acids are elongated polymers that are composed of linear segments of monomers. The monomers are called nucleotides and are comprised of three units referred to as a base, a sugar, and a phosphate group. The base is a nitrogen containing heterocyclic moiety that is either monocyclic or bicyclic. The monocyclic bases are called pyrimidines (**18**) and the bicyclic bases are called purines (**19**). The base is connected to the sugar, which is a five membered ring referred to as a pentose sugar. The sugar is then connected to a phosphate ester moiety. Nucleic acids are the basic building blocks for DNA and RNA.[23]

Pyrimidine (**18**)

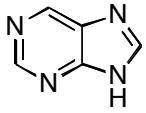

Purine (**19**)

Figure 6 General Structure of Nitrogenous Bases

2.3. The Components of DNA

DNA is essential to life since it contains all the cellular genetic material. It is composed of several smaller segments that are joined together to form a linear polymeric structure. These individual components include a base, a sugar, and a phosphate group.[22]

2.3.1. Bases

The bases of nucleic acids are often called nitrogenous bases since they are heterocyclic ring structures that contain several nitrogen atoms. Pyrimidines (**18**) and purines (**19**) make up the two classes of nitrogenous bases. Pyrimidines are made up of a six-membered heterocyclic ring. It contains two nitrogen atoms, is planar, and is aromatic. The two pyrimidines usually found in DNA include thymine (T, **20**) and cytosine (C, **21**). Purines are a fused heterocyclic ring composed of a pyrimidine and an imidazole. An imidazole is a five-membered, heterocyclic, aromatic ring that contains two nitrogen atoms. The fusion of these two rings results in a nine-membered, fused heterocyclic ring that contains four nitrogen atoms. The two purines usually found in DNA include adenine (A, **22**) and guanine (G, **23**).[22]

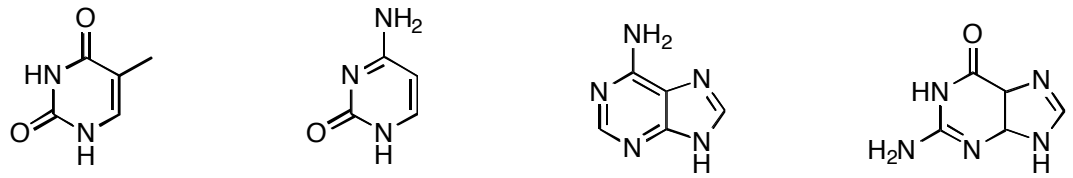

Thymine (**20**) Cytosine (**21**) Adenine (**22**) Guanine (**23**)

Figure 7 Structures of Nitrogenous Bases for DNA

2.3.2. Sugars

The sugar moiety in DNA is called a pentose since it is a five-carbon sugar. The sugar is a part of the furanose class of sugars since it is a ring formation of a ribose sugar (**24**), which is linear. The sugar used is DNA is D-2-deooxyribofuranose (**25**).[22]

2.3.3. Nucleosides

The link between a nitrogenous base and a sugar is called a glycosidic bond. This linked structure is called a nucleoside (**26**). The glycosidic bond joins the sugar's carbonyl carbon,

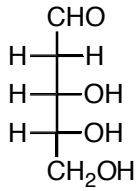

D-2-Deoxyribose (**24**)

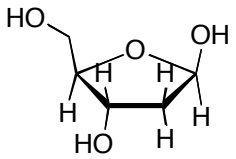

D-2-Deoxyribofuranose (**25**)

Figure 8 Structures of Sugars for DNA

which is also referred to as the anomeric carbon, to a nitrogen atom in the base. Since the bond is attached to a nitrogen atom in the base, it is specifically referred to as an *N*-glycosidic bond. Glycosidic bonds can exist as either a α or β conformation, with the β conformation being preferred. Nucleosides can also have varying conformations of the glycosidic bond. The conformation is determined by how the base is positioned relative to the anomeric carbon of the sugar. The two possible conformations are *syn* and *anti*. In the *syn* form for pyrimidines, the C-2 oxygen atom sits above the sugar and causes steric hindrance. Steric hindrance is absent in the *anti* form since the C-2 oxygen atom is turned away from the sugar ring. As a result, pyrimidine nucleosides prefer the anti conformation. The smaller purine nucleosides produce less steric hindrance and can exist in either a *syn* and *anti* conformation.[22]

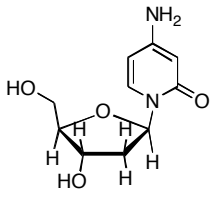

Nucleoside (**26**)

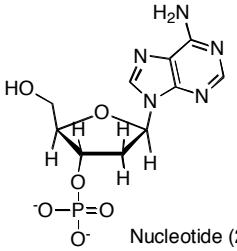

Nucleotide (**27**)

Figure 9 Structures of a Sample Nucleoside and Nucleotide

2.3.4. Nucleotides and Polynucleotides

A nucleotide (**27**) is comprised of a nitrogenous base, a pentose sugar, and a phosphate group. It is formed when phosphoric acid is added to a hydroxyl group of a sugar contained in a nucleoside creating an ester linkage.[22]

A polynucleotide, or nucleic acid, is an array of individual nucleotides that have been linked by phosphodiester bridges in a 3' to 5' arrangement. The nucleic acid formation occurs when the 5' phosphate of a nucleotide adds to the 3' hydroxyl of another nucleotide. When the nucleic acid is composed of deoxyribonucleotides, the polymer is called deoxyribonucleic acid, or DNA.[22]

2.4. DNA

DNA exists as a double helix structure that is created when two nucleic acid strands twist around each other. The two nucleic acid strands run in an antiparallel fashion and are held together by hydrogen bonding. The hydrogen bonding causes the nucleotide bases of one strand to complement the nucleotide bases of the opposite strand. This complementarity of the bases is called base pairing. The concept of base paring arose from the discovery by Edwin Chargaff of the composition of bases. In the 1940's, he found that the four bases do not occur in equal amounts in DNA. Actually, two pairs of bases always occur in equivalent amounts and that pyrimidines (**18**) always equal purines (**19**). These discoveries lead to what is now known as Chargaff's rules. Chargaff's rules states that the number of adenine (**22**) and thymine (**20**) residues are equivalent, the number of cytosine (**21**) and guanine (**23**) residues are equivalent, and the number of pyrimidines and purines are equivalent.

Using Chargaff's rules, James Watson and Francis Crick were able to deduce that the DNA double helix was complementary. They found that the hydrogen bonds that held the

strands together occurred between specific bases pairs of opposite strands such that one base was a pyrimidine and the other was a purine. Specifically they found that adenine always paired with thymine (A:T, **28**) and that guanine always paired with cytosine (G:C, **29**).[22]

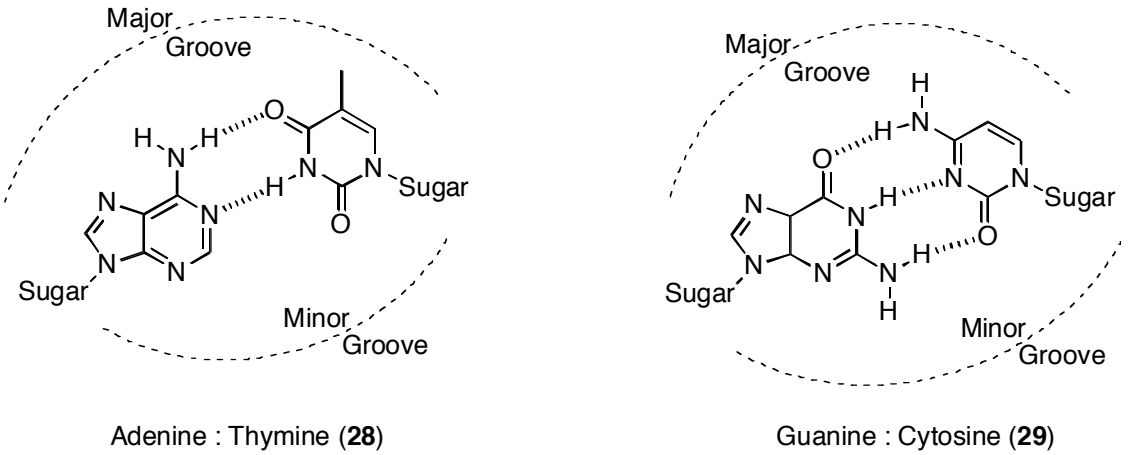

Adenine : Thymine (**28**) Guanine : Cytosine (**29**)

Figure 10 A:T and G:C Base Pairs with Major and Minor Groove

2.4.1. Common DNA Secondary Structures

Generally, DNA can exist is one of three secondary structures. These three forms are A, B, and Z DNA. DNA has two antiparallel strands that twist upon each other in a helical formation. The helix is held together by hydrogen bonding between the bases on the opposing strands and the base stacking results in a hydrophobic center. This arrangement causes the backbone of the chains, which consists of the sugar and the phosphate groups, to lie outside the helix. The helical nature of the structure causes the spacing between individual base pairs to be 0.34 nm and since the helix repeats every 10 base pairs, the pitch of the helix is 3.4 nm. This major conformation of DNA is referred to as B-DNA.[22] B-DNA dominates when in a fully hydrated state.[24]

The two backbones of the DNA are not equivalently spaced with regards to the helical axis of the DNA strand. This causes the two grooves to not be of the same width. As illustrated

in Figure 10, if the glycosidic bonds are in the downward position, then the groove that lies above the base pair is the larger, or major, groove and the smaller, or minor, groove lies below the base pair (**28**, **29**). [22] The major and minor grooves do have equal widths, or depths.[24]

An alternate form of DNA is A-DNA. A-DNA has a pitch of 2.46 nm and has an 11 base pair turn. The base pairs have a 19^{o} tilt with respect to the helical axis and the distance between base pairs is 0.23 nm.[22] The tilt of the base pairs causes the major groove to be very deep and the minor groove to be rather shallow.[24] These changes and the fact that the base pairs are placed around the helical axis cause A-DNA to be short and squat as compared to B-DNA.[22] A-DNA dominates when in dehydrated nonphysiological conditions.[24]

Z-DNA differs from both A and B DNA in that it is a left-handed helix instead of a right hand helix and that the guanosine residues are *syn* instead of *anti*. Z- DNA has a 12 base pair turn and a rise of 0.38 nm. The pitch of Z-DNA is 45.6 nm and these changes cause it to be long and thin as compared it B-DNA.[22] Z-DNA got its name from the fact that the backbone comprised of the sugar and phosphate groups have a zigzag pattern.[24]

2.4.2. G-Quadruplexes

Guanine residues have the ability to self-associate as a result of its ability to hydrogen bond using both Watson-Crick and Hoogsteen hydrogen bonding.[25] A G-quartet occurs when four guanine residues hydrogen bond amongst themselves to form a cyclic arrangement (Figure 11). Multiple G-quartets can stack on top of one another to create a class of secondary structures called G-quadruplexes.[26] G-quardruplexes can be formed by an intramolecular or an intermolecular arrangement. In the intramolecular formation (Figure 12), one guanine-rich DNA sequence is folded to form the G-quadruplex but in the intermolecular form (Figure 13), either two or four different sequences are used. Since single-stranded DNA sequences are involved,

the strands can run in a combination of parallel and anti-parallel directions. The folding pattern of the stands also cause the loops of several residues in length to form around the quadruplex and their location depends on the number of stands involved. If two stands run parallel to each other, then the loop occurs in the groove but if the strand runs antiparallel then the loop exists above or below the plane of the G-quartet.[25]

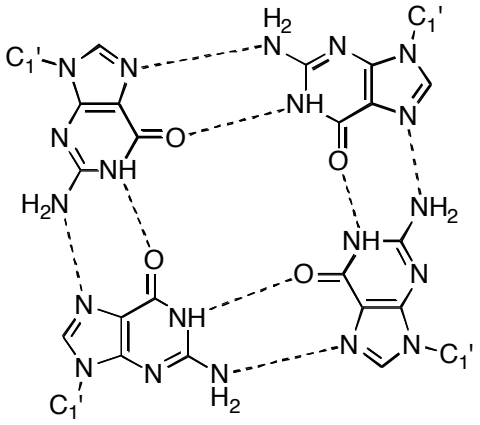

Figure 11 Arrangement of Guanine Bases to form a G-quartet

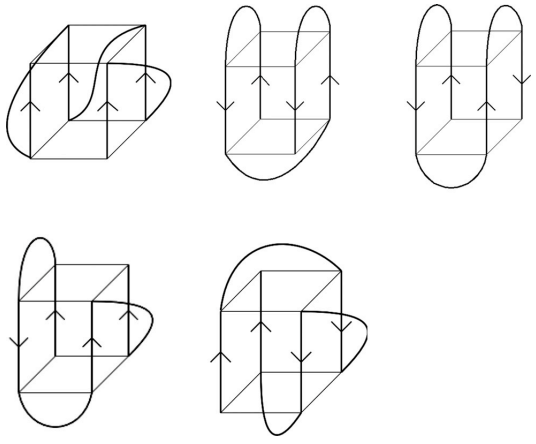

Figure 12 Examples of Intramolecular Topology Diagrams of G-quadruplexes[27]

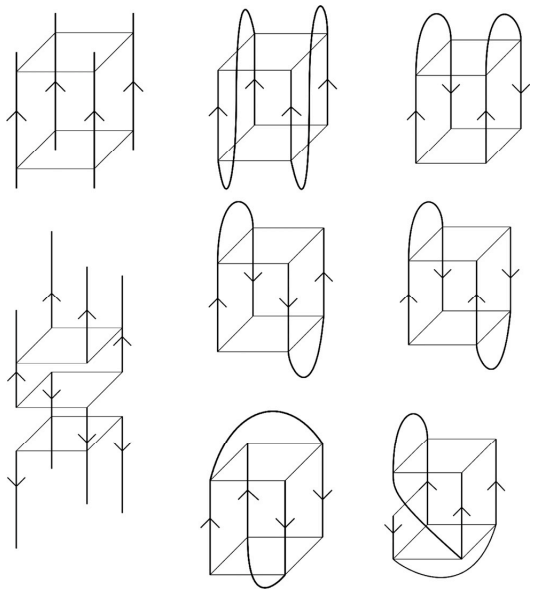

Figure 13 Examples of Intermolecular Topology Diagrams of G-quadruplexes[27]

2.5. DNA Binding

Several classes of drugs exist that interact with DNA. They are alkylators, strand breakers, and reversible binders. Alkylators are molecules that form a covalent interaction with DNA bases and strand breakers are molecules that create radicals that cleave the DNA strands. Reversible binders are molecules that can interact with DNA using reversible, noncovalent interactions. Reversible binding modes includes groove binding and intercalation.[20]

2.5.1. Alkylators

Alkylators are drugs that will irreversibly bind to DNA thru the formation of covalent bonds. Alkylation occurs when an atom is replaced with an alkyl group. This generally occurs by way of a nucleophilic substitution reaction with nitrogen, oxygen or sulfur nucleophiles and an eletrophilic alkylating agent. Problems with the use of alkylators include the toxicity due to

the non-selective alkylation and drug resistance since the cell ultimately decreases uptake of the drug and/or increases repair of the damage caused by the drug.[20]

2.5.2. Strand Breakers

Strand breakers are able to create radicals, which then remove hydrogen atoms from either the sugar-phosphate backbone of DNA or from the bases. The removal of the hydrogen atoms causes the strand of DNA to break.[20]

2.5.3. Minor Groove Binding

Small molecules can bind to the minor groove of the DNA. These molecules usually have aromatic ring systems attached with single bonds such that there is the ability to rotate in the groove. The A-T rich areas of the groove are slightly smaller than the G-C rich regions, so for many small molecules the preference is for A-T rich areas since they can provide a tighter fit in the minor groove. The small molecules that prefer binding to the A-T rich regions of the DNA strand are generally crescent-shaped and with NH groups on the internal part of the crescent.[20]

2.5.4. Intercalation

Intercalation occurs when a flat aromatic or heteroaromatic molecule gets inserted between the base pairs of helical DNA. The intercalating molecule ends up being stacked perpendicular to the helical axis. As a result, the remaining base pairs undergo a vertical shift and are separated. This causes the backbone to be modified and lengthens the DNA duplex. An intercalator can bind to every other base pair at most since the binding at one site disrupts the ability of a second intercalator to bind to an adjacent site due to a change in the conformation of

the duplex. Intercalation ultimately causes the unwinding of the DNA stand and most intercalators exhibit a preference for G-C rich sites in the helix.[20]

3. SYNTHESIS

3.1. Rationale Behind the Synthetic Strategy

Parasitic diseases have been estimated to affect over a billion people worldwide. Over 60 million people are at risk of getting infected with human African trypanosomiasis.[28] This number is steadily growing as the number of international travelers increase. While there are several drugs currently in use, there is a great need for the development of new treatments due to the lack of drug availability, production costs of current drugs, the difficult routes of drug administration, and drug toxicity and resistance.[2, 5]

There are several approaches for the development of new drugs for the treatment of human African trypanosomiasis. They include the creation of new formulations for currently used drugs, the use of new drug combinations, and the development of new drugs.[4] It is my intent to use the latter method in my research.

The prototypical diamidine, pentamidine (**8**), has been in use for over 50 years for the treatment of human African trypanosomiasis. Throughout this dissertation, diamidine structures are shown as a free base; however, when in biological systems, they are protonated and are dications. Unfortunately, the mechanism of action for the diamidine class of compounds has yet to be definitively elucidated. Research has shown that the compounds bind to the minor groove of DNA. It is thought that the binding to AT rich regions of the DNA helix is the crucial first step in their mode of action.[2] The key characteristics required for effective minor groove binders include the cationic centers at the terminus of the compounds, molecular flexibility, the ability to hydrogen bond, and a crescent shape of the molecule that is complementary to the minor groove.[29]

The center moiety of several previously synthesized diamidines has been a single heterocyclic ring. It is thought that the binding affinity of the molecules to DNA can be maintained or increased by elongation of the center moiety. As a result, my research has centered on the synthesis of molecules that have a center moiety composed of a fused heterocyclic ring. The compounds are intended to be a class of novel linear diamidines since recent literature has shown that linear diamidines exhibit both significant antiparasitic activity and acceptable binding affinity to the minor groove of DNA. Although these novel compounds lack the curvature that is generally thought to be required for adequate binding to the DNA minor groove, it has been shown that one or more water molecules can be involved in the DNA complex. It has been shown that the binding of the water molecule between the drug and the DNA, in effect, provides the necessary curvature.[30]

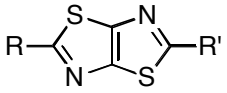

Thiazolothiazole (**30**)

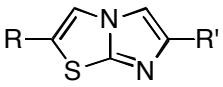

Imidazothiazole (**31**)

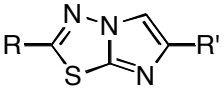

Imidazothiadiazole (**32**)

Figure 14 General Structures of a Thiazolothiazole, Imidazothiazole, and Imidazothiadiazole

3.2. Proposed Fused Heterocyclic Moieties

Several fused heterocyclic moieties were of synthetic interest. The first was a thiazolothiazole (**30**). The synthesis of the 2,5-diamidinophenyl parent compound was successful and two derivatives were also made. A second proposed structure was that of an imidazothiazole (**31**), which was intended to have a 2,5-diamidinophenyl substitution. The synthesis of this parent molecule was not achieved since attempts at cyclization procedures were not successful. The third proposed structure for synthesis was that of an imidazothiadiazoles

(**32**). The synthesis of this 2,5-disubstituted parent compound was unsuccessful due to the inability to convert the bromine atom to a cyano group to yield the biscyano prerequisite for amidine formation

3.3. Thiazolo[5,4-d]thiazoles

Johnson and Ketcham were interested in some synthetic work done by Ephraim in the 19th century. The work was of interest since Ephraim did not have structural evidence to prove that the proposed structure for 2,2'-diphenyl-4,4'-bithiazetime was correct. Ephraim's proposed structure (**33**) is that of two 4-membered rings joined together but Johnson and Ketchum thought that a structure composed of two fused 5-membered rings was more appropriate. Through a series of experiments, Johnson and Ketchum were able to deduce that the correct structure was that of the two fused 5-membered rings, known as a thiazolo[5,4-d]thiazole (**30**).[31] Several papers have been published which illustrate the synthesis of the parent compound and its derivatives though a condensation reaction with dithiooxamide and an aromatic aldehydes.[31-33] Some of the thiazolo[5,4-d]thiazole derivatives have been tested for their liquid crystal properties while others have tested as semiconductors.[34, 35]

33 Thiazolothiazole (**30**)

Figure 15 Proposed and Actual Structure of Thiazolo[5,4-d]thiazole

3.3.1. 2,5-Bis(4-cyanophenyl)thiazolo[5,4-d]thiazole (**36**)

For the synthesis of the parent 2,5-diarylthiazolo[5,4-d]thiazole, the first step involved the condensation of p-cyanobenzaldehyde (**34**) with dithiooxamide (**35**) in DMF (**Scheme 1**).

The mixture was allowed to reflux for 24 h. The crude solid was then recrystallized from DMF to yield 2,5-bis(4-cyanophenyl)thiazolo[5,4-d]thiazole (**36**).[33]

Scheme 1 Synthesis of 2,5-bis(4-cyanophenyl)thiazole[5,4-d]thiazole (36)

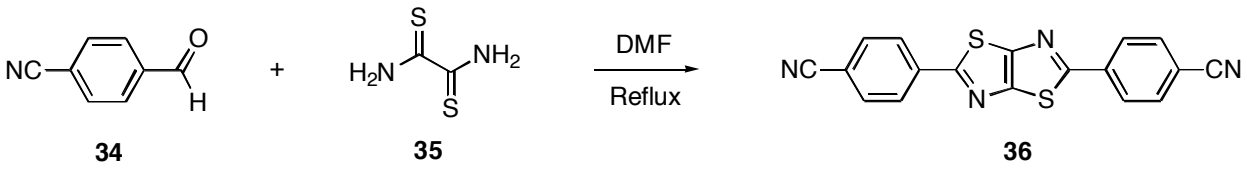

The formation of the thiazolothiazole (**36**) is thought to involve a multiple step process. A proposed mechanism is presented in scheme 2.

Scheme 2 Proposed mechanism for 2,5-bis(4-cyanophenyl)thiazole[5,4-d]thiazole (36)

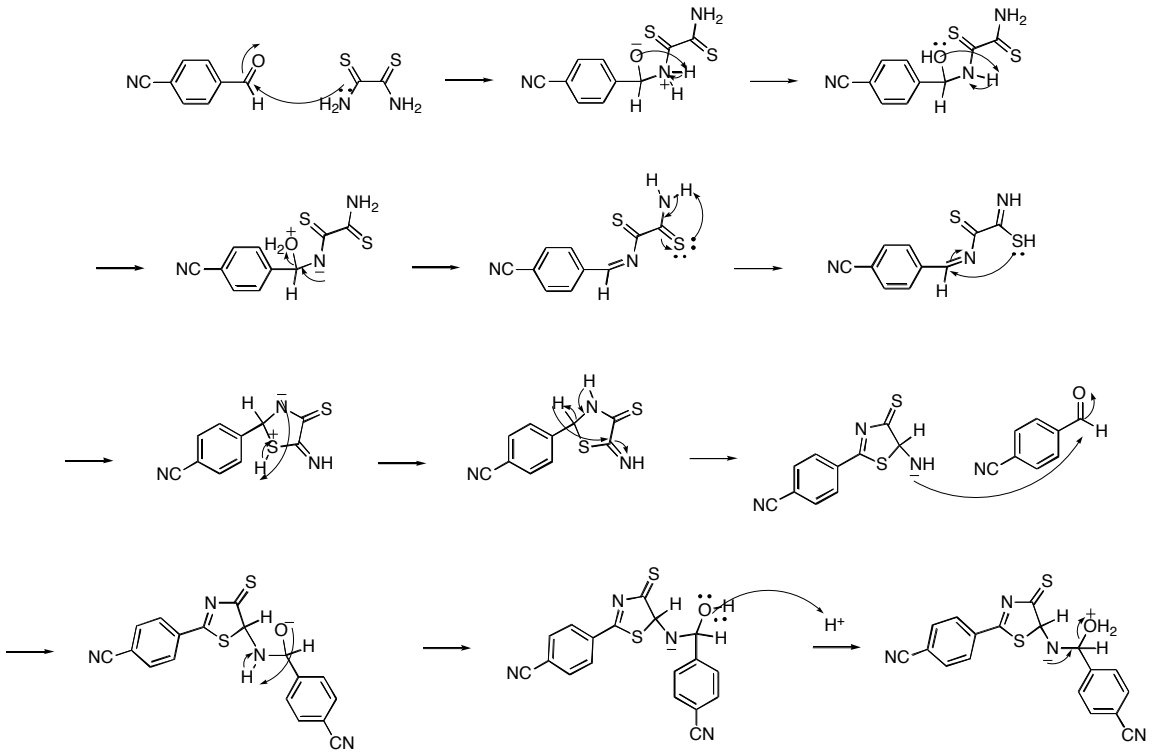

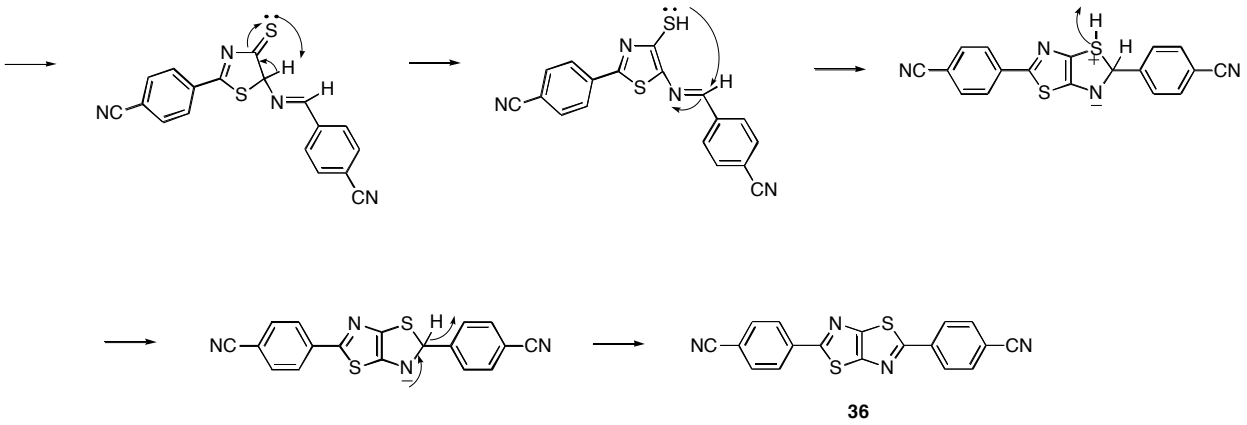

36

3.3.2. 2,5-Bis(4-amidinophenyl)thiazolo[5,4-d]thiazole HCl salt (**37, DB 1929**)

For the conversion of 2,5-bis(4-cyanophenyl)thiazolo[5,4-d]thiazole (**36**) into an amidine, the compound was allowed to react with lithium bis(trimethylsilyl)amide in THF (**Scheme 3**). Due to the low solubility of the bis-nitrile, the mixture was stirred at room temperature for several days until completely dissolved. The solution was cooled and EtOH-HCl was added. About a day later, the solvent was evaporated and ether was added. The mixture was then filtered, washed with ether, and dried. The dried solid was then suspended in H_2O and 10% NaOH was added until just basic. The mixture was then filtered, dried overnight, and suspended in an EtOH-MeOH mixture. The mixture was eventually filtered, washed and dried to yield 2,5-bis(4-amidinophenyl)thiazolo[5,4-d]thiazole as an HCl salt (**37, DB 1929**).[36]

Scheme 3 Synthesis of 2,5-bis(4-amidinophenyl)thiazole[5,4-d]thiazole HCl Salt (37)

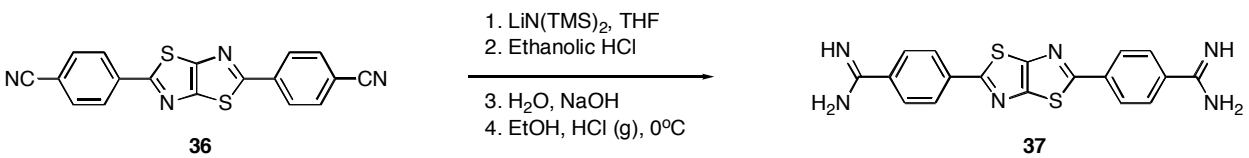

36 **37**

The conversion of the bisnitrile to the bisamidine by the action of lithium bis(trimethylsilyl)amide is straightforward. The possible mechanism is presented in scheme 4.

Scheme 4 Proposed mechanism for the conversion of a bisnitrile to an amidine

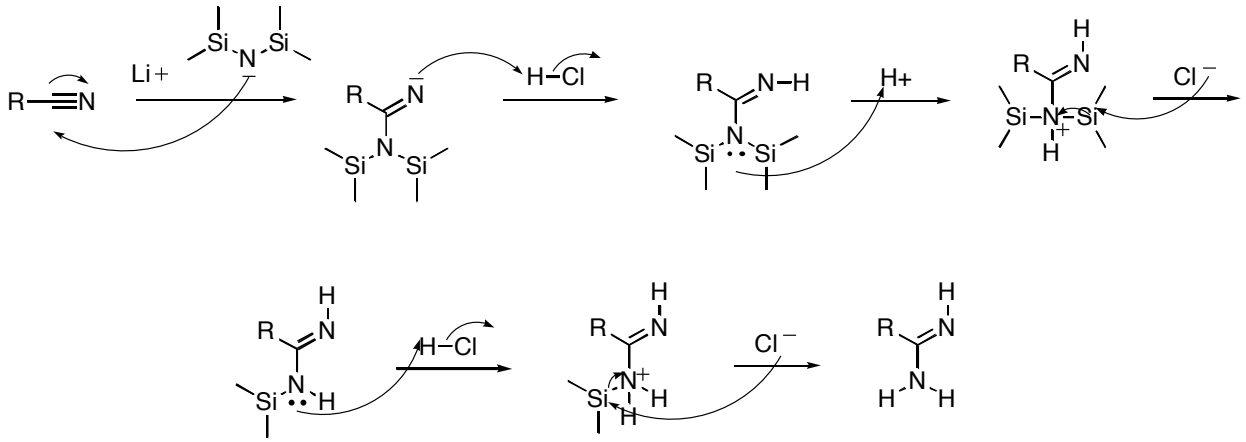

3.4. Derivatives of 2,5-bis(4-amidinophenyl)thiazolo[5,4-d]thiazole

The synthesis of several derivatives of 2,5-bis(4-amidinophenyl)thiazolo[5,4-d]thiazole (**37**) were attempted using the same method as that employed to make the parent compound but they were not successful. The first step to yield the fused heterocyclic molecule is where the problems were encountered. It was never possible to get a high enough conversion of starting material to product in the reactions or if an appreciable amount of product was present, it was extremely difficult to separate the product from the numerous by-products in the mixture. With these issues in mind, an alternative procedure for making thiazolo[5,4-d]thiazoles using o-dichlorobenzene as the solvent was used. This solvent was therefore used in subsequent reactions and was very successful.

3.4.1. 2,5-Bis(4-cyano-2-fluorophenyl)thiazolo[5,4-d]thiazole (**39**)

The first derivative to be synthesized was a fluoro derivative (**Scheme 5**). To make it dithiooxamide (**35**) was reacted with 4-cyano-2-fluorobenzaldehyde (**38**) in o-dichlorobenzene at reflux. After reflux, the mixture was cooled, filtered, and washed with ethanol to yield a crude solid. The crude solid was then boiled in DMF, hot filtered, and cooled to induce crystallization to yield 2,5-bis(4-cyano-2-fluorophenyl)thiazolo[5,4-d]thiazole (**39**).[33, 35]

Scheme 5 Synthesis of 2,5-bis(4-cyano-2-fluorophenyl)thiazole[5.4-d]thiazole (39)

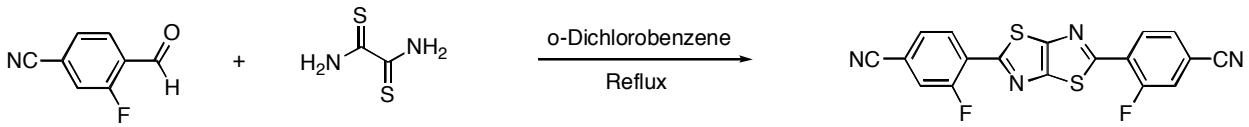

38 **35** **39**

3.4.2. 2,5-Bis(4-amidinophenyl-2-fluoro)thiazolo[5,4-d]thiazole HCl salt (**40**)

2,5-Bis(4-cyano-2-fluorophenyl)thiazolo[5,4-d]thiazole (**39**) was then converted into the amidine (**Scheme 6**) by the method previously described to yield 2,5-bis(4-amidinophenyl-2-fluoro)thiazolo[5,4-d]thiazole HCl salt (**40**).[36]

Scheme 6 Synthesis of 2,5-bis(4-amidinophenyl-2-fluoro)thiazole[5,4-d]thiazole HCl Salt (40)

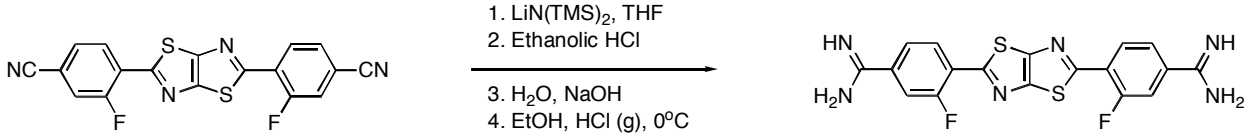

39 **40**

3.4.3. 2,5-Bis(4-cyano-2-methoxyphenyl)thiazolo[5,4-d]thiazole (**42**)

The second derivative that was synthesized was the methoxy derivative (**Scheme 7**). It was prepared with dithiooxamide (**35**) and 4-cyano-2-methoxybenzaldehyde (**41**) by the previously described method to yield 2,5-bis(4-cyano-2-methoxyphenyl)thiazolo[5,4-d]thiazole (**42**).[33, 35]

Scheme 7 Synthesis of 2,5-bis(4-cyano-2-methoxyphenyl)thiazole[5.4-d]thiazole (42)

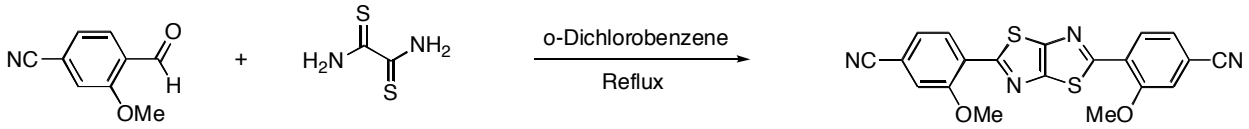

41 **35** **42**

3.4.4. 2,5-Bis(4-amidinophenyl-2-methoxy)thiazolo[5,4-d]thiazole HCl salt (**43**)

2,5-Bis(4-cyano-2-methoxyphenyl)thiazolo[5,4-d]thiazole (**42**) was then converted into the amidine (**Scheme 8**) as previously described to yield 2,5-bis(4-amidinophenyl-2-methoxy)thiazolo[5,4-d]thiazole HCl salt (**43**).[36]

Scheme 8 Synthesis of 2,5-bis(4-amidinophenyl-2-methoxy)thiazole[5,4-d]thiazole HCl Salt (43)

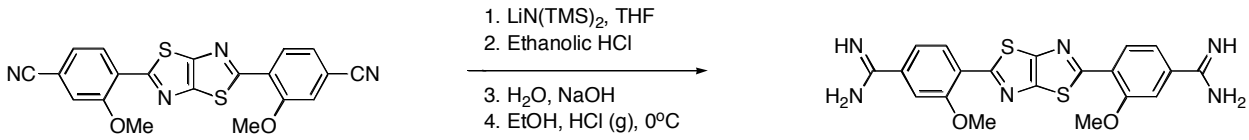

42 **43**

3.5. Novel Findings for DB 1929

The goal of this research was to synthesize a novel class of diamidines that consisted of a fused heterocycle as the center moiety in the hopes that the elongation of the distance between the two cationic ends would maintain or increase the binding affinity for the DNA minor groove as compared to other diamidines. This novel class of compounds employs the use of a thiazole[5,4-d]thiazole as the center motif and causes the molecule to be linear.

It was initially thought that diamidines needed to have a crescent shape that was complementary to the curve of the DNA minor groove for acceptable binding affinity.[37] Research has shown that linear diamidines can exhibit antiparasitic activity as well. Several terphenyl diamidines have displayed good binding affinity and antiparasitic activity.[38] A near-linear diamidine, DB 921, which is a biphenyl benzimidazole, uses a water molecule bound to one of the amidine ends to provide the necessary molecular curvature.[30, 37] The water molecule assists the amidine by acting as a bridge. The amidine hydrogen bonds to the water molecule and the water is then able to hydrogen bond to the floor of the minor groove. It is the use of the water that helps achieve the good binding affinity for DB 921.[39]

This data proved informative for my research since the use of a fused heterocycle, specifically thiazole[5,4-d]thiazole, as the center motif would create a novel class of linear diamidines that is expected to display reasonable binding affinity for the DNA minor groove. To date, the parent diamidine, 2,5-Bis(4-amidinophenyl)thiazolo[5,4-d]thiazole HCl salt (**37**) or DB 1929, and two derivatives have been synthesized. Biological data has been collected for the parent compound.

DB 1929 (**37**) underwent some biological testing that was performed by a collaborator, Reto Brun. The *in vitro* activity for *T. b. rhodesiense* was 77 nM (IC_{50}) and the cytotoxicity

measurement in L6 cells was 8.0 μM (IC_{50}). This data is promising since it shows that DB 1929 is highly selective for trypanosomiasis, that it is a good candidate for animal studies, and a good candidate for optimization.

The biological data for the two derivatives of DB 1929, a fluoro compound (**40**) and a methoxy compound (**43**) have yet to be completed and will be published at a later date.

DB 1929 has also been shown to bind to G-quadruplexes, based on the experiments done by a collaborator, Caterina Musetti.[40] Several measurements were taken that enable one to arrive at this conclusion. For starters, a circular dichroism (CD) experiment was performed with human telomere G-quadruplex. CD shows that binding of DB 1929 causes a conformational change in the quadruplex. The quadruplex changes from a parallel to an anti-parallel arrangement. This conformational change is illustrated in Figure 16 by the peak at about 375 nm since the peak increases as the concentration of the compound increases.

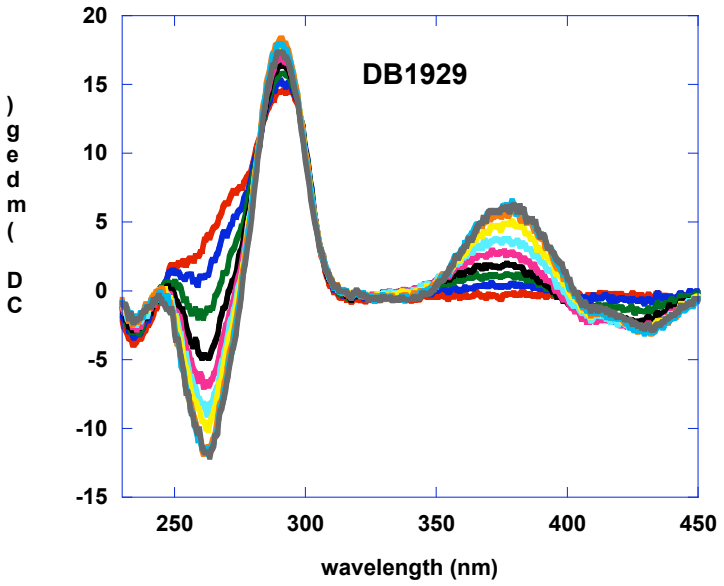

Figure 16 CD Titration of DB 1929 with Human Telomere G-quadruplex [40]

Surface plasmon resonance (SPR) was also used to determine if DB 1929 binds to the G-quadruplex. In this instance, DB 1929 was measured with human telomeres and with c-myc. In the sensograms of Figure 17, the response increases as the concentration of the compound increases and shows that DB 1929 binds to both the human telomere and to c-myc.

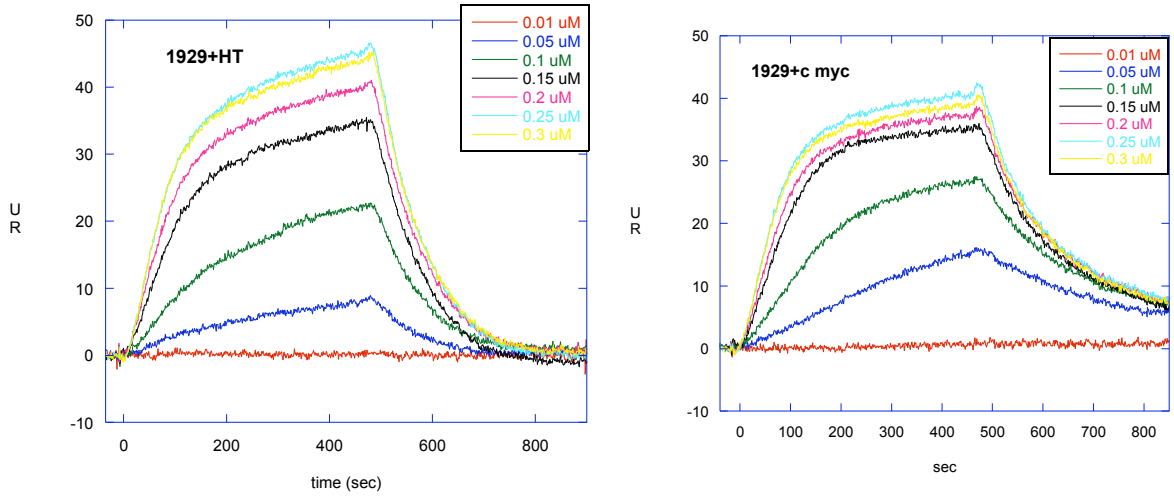

Figure 17 SPR Titration Curves for DB 1929 with Human Telomeres and C-Myc [40]

To prove that the binding of DB 1929 to the G-quadruplex was selective, SPR was done with the DNA duplex (Figure 18). The sensorgram produced from this experiment did not display a considerable response increase as the concentration of the compound increased. This is evidence that DB 1929 selectively binds to the G-quadruplex over that of the DNA duplex.
A summary of the SPR data is in Figure 19. It is a best-fit plot of the response unit (ru) values from the steady-state region of the sensorgrams against the concentration of unbound DB 1929 from the three previous sensorgrams. This figure further illustrates the selectivity of DB1929 for the G-quadruplex over the DNA duplex. Binding constants were determined from the sensorgrams and are in Figure 20. The figure shows that there are two binding constants for both the human telomere G-quadruplex and c-myc. Human telomere G-quadruplex has a similar

binding affinity for both binding sites and the second binding affinity is lower than the first for c-myc.

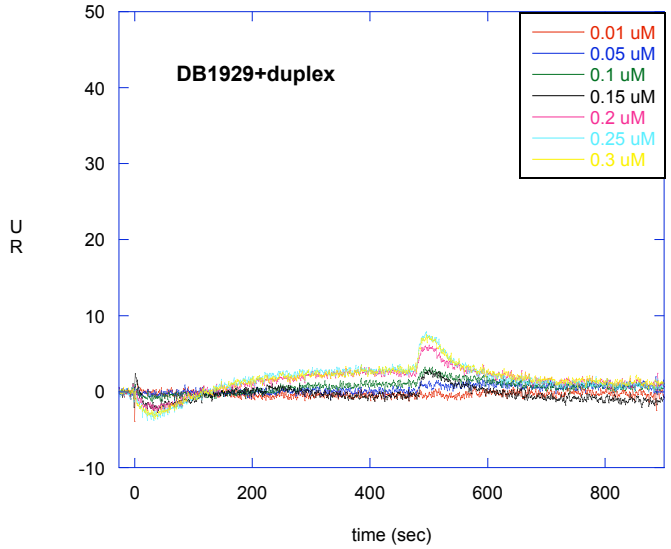

Figure 18 SPR Titration Curve for DB 1929 with Duplex DNA [40]

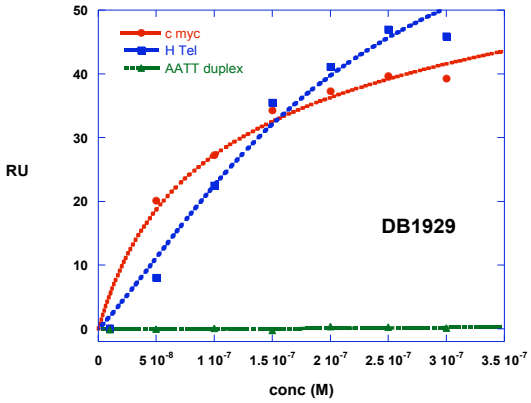

Figure 19 Best Fit Plot of Data from Steady State Region of SPR Sensorgrams [40]

	H Tel quadruplex	*c myc* quadruplex	AATT duplex
DB 1929	$4.8*10^6\ M^{-1}$ $5.1*10^6\ M^{-1}$	$1.6*10^7\ M^{-1}$ $9.1*10^5\ M^{-1}$	- -

Figure 20 Binding Constants From SPR [40]

In addition to the biological data, DB 1929 was tested for the possibility of fluorescence and is compared to DB 75 (Table 1). These two compounds provided an excitation wavelength range of 359-368 nm and an emission wavelength range of 453-466 nm. DB 75 has an excitation wavelength of 359 nm and an emission wavelength of 466 nm. DB 1929 has an excitation wavelength that is 9 nm higher at 368 nm and an emission wavelength that is 13 nm lower at 453 nm, as compared to DB 75. The emission intensity of DB 1929 is significantly lower at 11 au as compared to a value of 295 au for DB 75. Both compounds fluoresce in the blue region of the visible spectrum. A further discussion on fluorescence of diamidines follows in chapter 4.

Table 1 Comparison of DB 75 and DB 1929

DB #	Excitation λ max (nm)	Emission λ max (nm)	Emission Intensity (au)	Structure
75	359	466	295	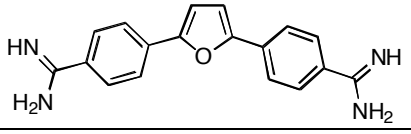
1929	368	453	11	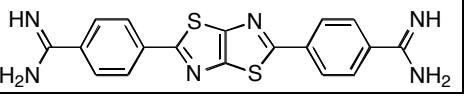

Note: All data is uncorrected and fluorescence measurements were taken at excitation slitwidth of 2.5 and an emission slitwidth of 5. Excitation concentration is 1.66 μM to 16.66 μM and emission concentration is 1 μM.

A collaborator, Catharine Collar, performed molecular modeling of the thiazolothiazole compounds. The energy minimization calculations were performed to detect the torsional angles of the compounds. The results showed that the phenyls and fused heterocycle are planar with the amidines rotated approximately 60^{o} or 120^{o}.

Figure 21 provides a visual representation of the molecules. The top row is DB 1929, which has unsubstituted phenyl groups. The second row is the fluoro derivative and the third

row is the methoxy derivative. The left-handed column of Figure 21 is sighted along the amidine carbon to phenyl carbon bond and shows that the amidines are rotated as compared the rest of the structure. The right-handed column shows that the phenyls and fused thiazolothiazole are planar.

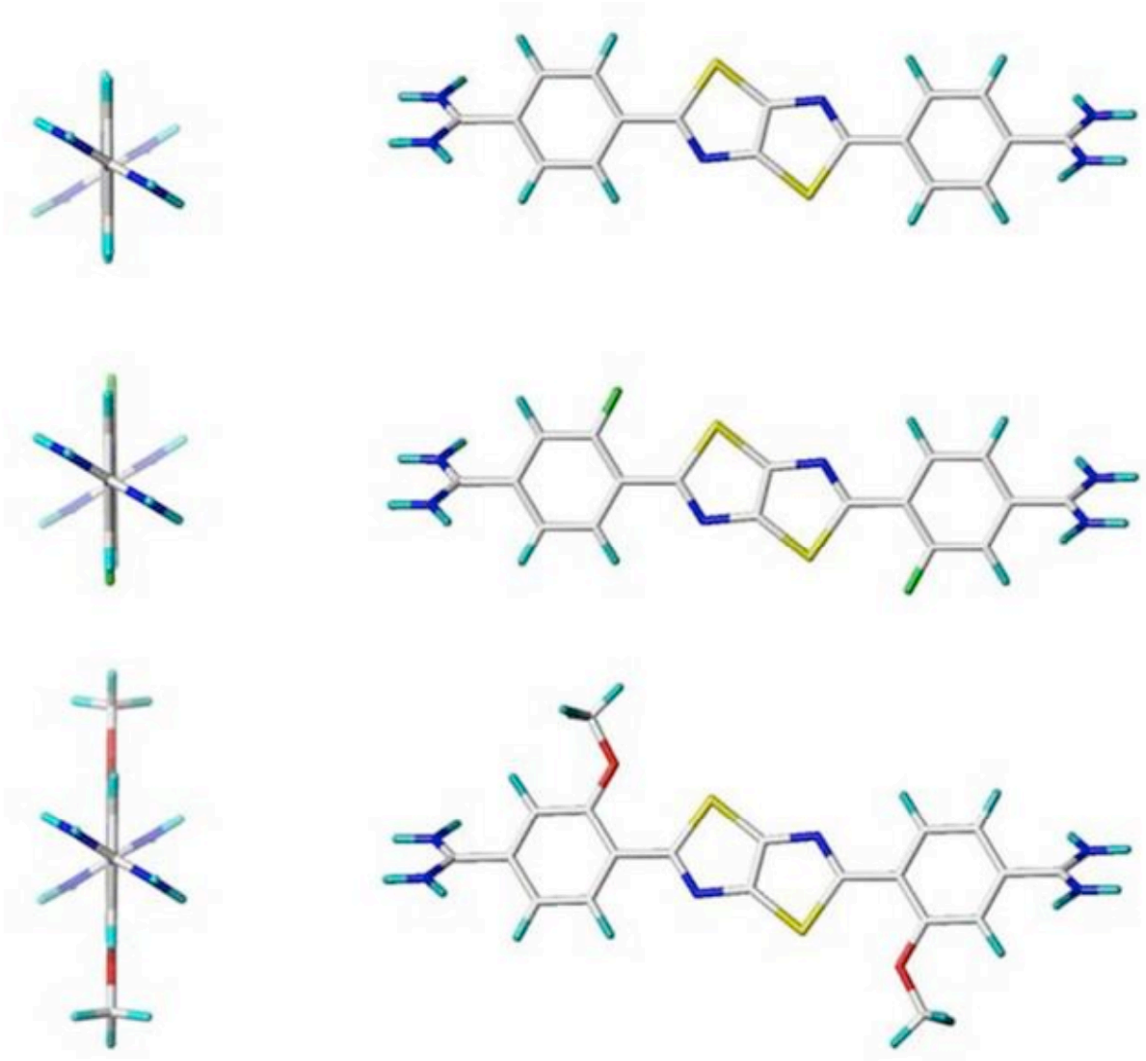

Figure 21 Lowest energy conformations for DB1929 (Top), fluorine Derivative (Center), and methoxy derivative (Bottom)

3.6. Conclusions

A novel class of linear diamidines with a fused heterocycle as the center moiety has been synthesized. The parent diamidine, 2,5-Bis(4-amidinophenyl)thiazolo[5,4-d]thiazole HCl salt

(**37**) or DB 1929, has exhibited high *in vitro* activity for *T. b. rhodesiense* and low cytotoxicity L6 cells. This data demonstrates that DB 1929 is selective for trypanosomiasis. DB 1929 has also been shown to selectively bind to human telomere G-quadruplexes over duplex DNA. As a result, these thiazole[5,4-d]thiazole molecules are promising for further study of drug candidates for the treatment of Human African Trypanosomiasis.

3.7. Experimental

Melting points were determined using a Mel-Temp 3.0 capillary melting point apparatus and are uncorrected. IR was recorded on a Perkin Elmer Spectrum One spectrometer. Analytical TLC was performed on Whatman flexible silica gel plates containing fluorescent indicator on aluminum backing to monitor reactions. TLC visualization was done with UV light. ^{1}H and ^{13}C NMR spectra were recorded using a Bruker Avance 400 instrument and the δ are in ppm relative to TMS and coupling constants are in Hertz. Typical proton and carbon NMR spectra are found in the appendix. Elemental analysis was obtained from Atlantic Microlab, Norcross, GA. Mass spectrometry was obtained from the GSU Mass Spectrometry Facility, Atlanta, GA. Reagents were purchased and used without further purification from Sigma-Aldrich, Acros Organics, Lancaster, Alfa Aesar, Frontier Scientific, and Carbocore.

2,5-Bis(4-cyanophenyl)thiazolo[5,4-*d*]thiazole (**36**)

4-Cyanobenzaldehyde **34** (7.05 g, 54 mmol), dithiooxamide **35** (3.01 g, 25 mmol), and DMF (50 ml, anhydrous) were added together under a nitrogen atmosphere with stirring. The mixture was heated to reflux. After 24 h at reflux, the red-orange mixture was cooled to room temperature. Once cool, the precipitate was filtered, washed with EtOH, and allowed to air dry

overnight to yield crude **36** (4.85 g) as an orange solid. The crude sample was recrystallized in DMF (~1L). After 3 days, the mixture was filtered, washed with DMF, and dried overnight under vacuum to yield **36** (5.11 g, 15 mmol, 59%) as a yellow solid: mp 360.0-361.4^{o}C, lit. 354-55^{o}C; ^{1}H NMR (100 MHz, $CDCl_3$) δ (ppm) 8.10 (4H, d, J = 8.4Hz), δ 7.76 (4H, d, J = 7.6 Hz); Anal. Calcd for $C_{18}H_8N_4S_2$: C 62.77, H 2.34, N 16.27; Found C 62.75, H 2.32, N 16.25.

2,5-Bis(4-amidinophenyl)thiazolo[5,4-*d*]thiazole HCl Salt (**37, DB 1929**)

2,5-Bis(4-cyanophenyl)thiazolo[5, 4-*d*]thiazole (**36**) (0.34 g, 0.99 mmol) was added to THF (10 ml, anhydrous) under a nitrogen atmosphere with stirring at room temperature. Lithium bis(trimethylsilyl)amide (8.00 ml of 1.0 M in THF) was then added drop wise. The mixture was allowed to stir until completely dissolved. After 3 days, the flask containing the transparent red-brown solution was cooled to 0^{0}C for 30 min. The solution was made slightly acidic by the drop wise addition of an saturated EtOH-HCl solution (~3 ml) and allowed to stir in the ice bath overnight. Following overnight stirring, the yellow mixture was concentrated, suspended in anhydrous ether, and allowed to stir at room temperature for 30 min. The mixture was then filtered and washed with ether. The yellow solid was then dried under vacuum at 50^{0}C for 15 min.

The crude salt was then converted into the free base by suspending it in H_2O (~1 ml), placing it in an ice bath, and adding NaOH (10%) dropwise until the solution was slightly basic. The orange mixture was then filtered with cold H_2O and stored overnight in a vacuum desiccator. The resulting orange solid was suspended in a 50:50 EtOH-MeOH mixture and allowed to stir for 10 min. For conversion into the HCl salt, saturated EtOH-HCl (~1 ml) was added and the

mixture was allowed to stir overnight at room temperature. The precipitate was filtered and washed with ether and allowed to dry overnight in a vacuum desiccator to yield **37 (DB 1929)** (0.355 g, 0.738 mmol, 75%) a yellow solid: mp 354.2-356.4^{o}C; ^{1}H NMR (100 MHz, d_6-DMSO) δ (ppm) 9.34 (6H, s, NH), δ 8.29 (4H, d, J = 8.4 Hz); δ 8.03 (4H, d, J = 8.4 Hz); ^{13}C NMR (400 MHz, d_6-DMSO) δ (ppm) 168.2, 165.2, 152.4, 137.7, 130.6, 129.9, 127.0; MS-ESI calcd m/z 378.48, found m/z 379.2 [M+H]; Anal. Calcd for $C_{18}H_{14}N_6S_2$*2 HCl*1 H2O*0.25 CH_3CH_2OH: C 46.20, H 4.09, N 17.47; Found C 46.25, H 3.99, N 17.10.

2,5-Bis(4-cyano-2-fluorophenyl)thiazolo[5,4-*d*]thiazole (**39**)

4-Cyano-2-fluorobenzaldehyde **38** (1.62 g, 11 mmol) and dithiooxamide **35** (0.51 g, 4 mmol) were suspended in *o*-dichlorobenzene (15 ml) under a nitrogen atmosphere and heated at reflux with stirring. After 24 h at reflux, the mixture was cooled, filtered, and washed with cold EtOH. The resulting solid was then dried under vacuum to yield crude **39** (0.84 g) as a brown solid. The crude solid was then suspended in DMF, boiled for about 6 h, and filtered hot. Once cooled, crystallization was induced with the use of an ice bath. Four days later, the resulting solid was filtered and washed with cold DCM followed by being dried under vacuum with heat (~100^{o}C) to yield **39** (0.47 g, 1.24 mmol, 29%) as brown solid: mp 384.3-386.8^{o}C; ^{1}H NMR (100 MHz, d_6-DMSO) δ (ppm) 8.439 (1H, t), δ 8.145 (1H, d, J = 11.6 Hz); δ 7.907 (1H, d, J = 7.6 Hz); IR (cm^{-1}) 2240, 1564, 1118, 898, 801; Anal. Calcd for $C_{18}H_6N_4S_2F_2$: C 56.83, H 1.59, N 14.73; Found C 56.79, H 1.60, N 14.52.

2,5-Bis(4-amidinophenyl -2-fluoro)thiazolo[5,4-*d*]thiazole HCl Salt (**40**)

2,5-Bis-(4-cyano-2-fluorophenyl)thiazolo[5, 4-*d*]thiazole (**39**) (0.40 g, 1.05 mmol) was added to THF (10 ml, anhydrous) under a nitrogen atmosphere with stirring at room temperature. Lithium bis(trimethylsilyl)amide (9.00 ml of 1.0 M in THF) was then added drop wise. The mixture was allowed to stir until completely dissolved. After a week, the mixture had not dissolved so a second addition of THF (5 ml) and lithium bis(trimethylsilyl)amide (10.00 ml) were added with continued stirring at room temperature. About 4 days later, a third addition of lithium bis(trimethylsilyl)amide (10.00 ml) was added. A week later a forth addition of lithium bis(trimethylsilyl)amide (12.00 ml) was added and allowed to continue stirring at room temperature. After another 3 weeks or 7 weeks total, the mixture had become a red-brown solution. The flask containing the red-brown solution was then cooled to 0^0C for 30 min. The solution was made slightly acidic by the drop wise addition of a saturated EtOH-HCl solution (~4 ml) and allowed to stir in the ice bath overnight. Following overnight stirring, the mixture was concentrated, suspended in anhydrous ether, and allowed to stir at room temperature for 30 min. The mixture was then filtered and washed with ether. The light brown solid was then dried under vacuum at 50^0C for 15 min.

The crude salt was then converted into the free base by suspending it in H_2O (~15 ml), placing it in an ice bath, and adding NaOH (10%) dropwise until the solution was slightly basic. The orange mixture was then filtered with cold H_2O and stored overnight in a vacuum desiccator. The resulting brown solid was suspended in an 80:20 mixture of EtOH-MeOH (~18ml) and allowed to stir for 10 min. For conversion into the HCl salt, EtOH-HCl (~3 ml) was added until the suspension was slightly acidic and it was allowed to stir overnight at room temperature. The

precipitate was filtered, washed with EtOH and ether and allowed to dry overnight in a vacuum desiccator to yield **40** (0.45 g, 1.05 mmol, 84 %) as a yellow-brown solid: mp >400^{o}C; ^{1}H NMR (100 MHz, d_6-DMSO) δ (ppm) δ 8.357 (t), δ 7.978 (d, J = 8.4 Hz), δ 7.785 (t), δ 7.698 (d, J = 8.40 Hz), δ 7.280 (s); MS-ESI calcd 414.1 m/z, found 415.2 [M+H]; Anal. Calcd for $C_{18}H_{12}F_2N_6S_2$ * 1.3 HCl * 1.2 CH_3CH_2OH: C 47.38, H 4.00, N 16.25; Found C 47.48, H 3.61, N 15.86.

2,5-Bis(4-cyano-2-methoxyphenyl)thiazolo[5,4-*d*]thiazole (**42**)

4-Cyano-2-methoxybenzaldehyde **41** (1.77 g, 11 mmol) and dithiooxamide **35** (0.52 g, 4 mmol) were suspended in *o*-dichlorobenzene (80 ml) under a nitrogen atmosphere and heated at reflux with stirring. After 24h, the mixture was cooled, filtered, and washed with cold EtOH. The resulting solid was then dried under vacuum to yield crude **42** (1.04 g). The crude solid was then suspended in a 80:20 mixture of DMF-EtOH (~30 ml), boiled for about 4h and filtered hot. Once cooled, the mixture was filtered, washed with EtOH, and dried under vacuum with heat (~100^{o}C) to yield **42** (0.94 g, 2.32 mmol, 54%) as yellow solid: mp >400^{o}C; IR (cm^{-1}) 3087, 2949, 2226, 1751, 1562, 1279, 1016, 821; Anal. Calcd for $C_{20}H_{12}N_4S_2O_2$: C 59.39, H 2.99, N 13.85; Found C 59.20, H 2.84, N 13.84.

2,5-Bis(4-amidinophenyl-2-methoxy)thiazolo[5,4-*d*]thiazole HCl Salt (**43**)

2,5-Bis-(4-cyano-2-methoxyphenyl)thiazolo[5, 4-*d*]thiazole (**42**) (0.60 g, 1.49 mmol) was added to THF (10 ml, anhydrous) under a nitrogen atmosphere with stirring at room temperature.

Lithium bis(trimethylsilyl)amide (10.00 ml of 1.0 M in THF) was then added drop wise. The mixture was allowed to stir until completely dissolved. After a week, the mixture had not dissolved so a second addition of THF (5 ml) and lithium bis(trimethylsilyl)amide (10.00 ml) were added with continued stirring at room temperature. About 4 days later, a third addition of lithium bis(trimethylsilyl)amide (10.00 ml) was added. A week later a forth addition of lithium bis(trimethylsilyl)amide (12.00 ml) was added and allowed to continue stirring at room temperature. After another 3 weeks or 7 weeks total, the mixture had become a red-brown solution. The flask containing the red-brown solution was then cooled to 0^0C for 30 min. The solution was made slightly acidic by the drop wise addition of a saturated EtOH-HCl solution (~5 ml) and allowed to stir in the ice bath overnight. Following overnight stirring, the mixture was concentrated, suspended in anhydrous ether, and allowed to stir at room temperature for 30 min. The mixture was then filtered and washed with ether. The pale yellow solid was then dried under vacuum at 50^0C for 15 min.

The crude salt was then converted into the free base by suspending it in H_2O (~15 ml), placing it in an ice bath, and adding NaOH (10%) dropwise until the solution was slightly basic. The mixture was then filtered with cold H_2O and stored overnight in a vacuum desiccator. The resulting solid was suspended in an 80:20 mixture of EtOH-MeOH (~18ml) and allowed to stir for 10 min. For conversion into the HCl salt, saturated EtOH-HCl (~4 ml) was added until the suspension was slightly acidic and it was allowed to stir overnight at room temperature. The precipitate was filtered, washed with EtOH and ether and allowed to dry overnight in a vacuum desiccator to yield **43** (0.88 g, 1.49 mmol, 112 %) as a yellow-green solid: mp >400^{o}C; ^{1}H NMR (100 MHz, d_6-DMSO) δ (ppm) 7.287 (1H, s), δ 7.816 (1H, d, J = 8.4 Hz); δ 7.996 (1H, d, J = 8.4

Hz); MS-ESI calcd m/c 438.1, found m/z 439.3 [M+H]; Anal. Calcd for $C_{20}H_{18}O_2N_6S_2$ * 1.4 HCl * 0.9 CH_3CH_2OH: C 49.31, H 4.71, N 15.83; Found C 49.43, H 4.32, N 15.42.

Molecular Modeling

Compounds were constructed in SYBYL 8.1 and then minimized to convergence using the conjugate gradient method with a termination gradient of 0.001, Tripos force field, and Gasteiger-Huckel charges. Grid Search, of the Advanced Computation module in SYBYL, was then employed to systematically explore torsional freedoms and acquire the lowest energy conformations. All four torsional angles of the compounds were examined in full, 360°, through increments of 60 degrees. At each increment the bond is constrained and the conformation is minimized.

4. FLUORESCENCE

4.1. Introduction

The emission of light from an electronically excited molecule is a phenomenon known as luminescence.[41] The emission can be in the form of infrared, ultraviolet, or visible photons.[42] Many types of luminescence exist and they differ based on the excitation process. Luminescence that occurs with the excitation of a photon is therefore called photoluminescence. Photoluminescence can further be divided into fluorescence, phosphorescence, and delayed fluorescence.[42]

Fluorescence occurs from an excited singlet state. The electron in the excited state has an opposite spin as compared to that of the ground state. This occurrence is referred to as spin paired. The return of the excited electron to the ground state is therefore allowed and results in the emission of light, or a photon. Fluorescence generally occurs at a rate of 10^8 s^{-1}, so the lifetime is usually 10 ns. The lifetime of a fluorophore is the average time between the electron's excitation and its return to the ground state. The emission of a photon from the triplet excited state is known as phosphorescence. In this instance, the electrons in both the excited and the ground states have the same spin orientation (i.e. either both are spin up or spin down). The transition from the excited state to the ground state is therefore not allowed. The resulting emission of light is much slower at 10^3 to 10^0 s^{-1} and have lifetimes of milliseconds to seconds.[41]

Jablonski diagrams are the hallmark for the visual description of the absorption and emission of light. They are named after Alexander Jablonski, who is credited as being the father of fluorescence.[41] Figure 16 illustrates a typical Jablonski diagram. The electronic states are denoted S_0, S_1, and S_2,….S_n with the first being the ground state and the subsequent levels being

the excited states. S_n is used to abbreviate the fact that it is a singlet state, where n indicates that each electronic state is further subdivided into vibrational states and are labeled 0, 1, 2, and so forth. In the diagram, a vertical line is used to show the transitions between the different electronic states for the depiction of the light absorption. These transitions happen in a time frame of 10^{-15} s. This illustrates the Franck-Condon principle, which in a less complicated fashion simply means that the movement from one energy level to another is so fast that the atomic nuclei undergoing the transition are considered to be motionless during the transition.[41, 43] The transitions are the result of the excitation of the electrons and not the movement of the nuclei. The excitation process is almost instantaneous so it is not possible for the nuclei to alter their positions since they move at a slower rate as compared to the electrons.[42]

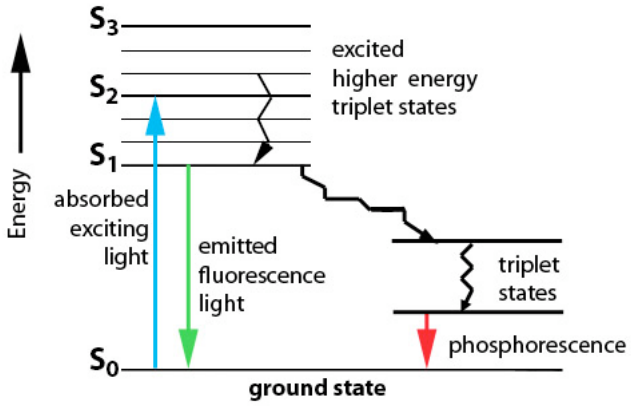

Figure 22 Jablonski Diagram[44]

During the process of absorption, the fluorophore, which is a fluorescent substance, is excited to a vibrational level of one of the excited states. Once absorption occurs, there is an option for the molecule to relax downward towards the lowest, or zero, vibrational level of S_1. This phenomenon is known as internal conversion.[41] Internal conversion is a non-radiative process that involves the release of energy.[42] Internal conversion is on the timescale of 10^{-12} s

and generally precedes emission since the lifetimes of a fluorescent molecule is 10^{-8} s. As a result, fluorescence usually occurs from the lowest vibrational level of S_1, which is a thermally equilibrated excited state.[41]

The next step for the fluorophore is the descent to the ground state. In general, the electron would have already undergone internal conversion and descended to the lowest lying vibrational level of the S_1 excited state. The fall of the electron from this level to any vibrational level in the ground state would generate light and is known as fluorescence.[42] On examination of a plot of the wavelength versus intensity, it can be seen that the emission spectrum resembles that of the absorption spectrum. This is due to a lack of change in the geometry of the molecule following the excitation and to the similarity in the spacing between the vibrational levels of both the ground and excited states. This is known as the mirror image rule and it is also substantiation that the molecule was not excited above the first excited state[45]. Stokes Rule says that the wavelength of the fluorescence emission ought to be higher that the absorption wavelength. Generally, the absorption and emission spectra will overlap since some of the light is actually emitted at a wavelength that is lower than the absorption wavelength.[42]

Figure 16 also displays the conversion of the molecule from the S_1 to the T_1, or triplet, state. This is known as intersystem crossing.[41] Intersystem crossing is a non-radiative process and occurs between vibrational levels of the S_1 and the T_1 states that are energetically equivalent.[42] The emission that occurs with the electrons descent from the T_1 excited state to the ground state is called phosphorescence. This happens at a much longer wavelength and therefore a lower energy as compared to fluorescence.[41] This process occurs in the microsecond (10^{-6} s) timescale and is therefore much slower than fluorescence. It should be noted that the transition from the T_1 state to the first vibrational level of the ground state is

forbidden thus causing the degree of emission to be significantly smaller than that of fluorescence.[42]

Delayed fluorescence is the transition from T_1 to S_1, which is reverse intersystem crossing. This process happens when the energy difference between the two excited states is small. The emission that occurs when the electron returns to the ground state following the reverse intersystem crossing is just like the normal fluorescence except it has a longer time constant.[42]

While phosphorescence and delayed fluorescence are important phenomena, they were not examined in this dissertation.

For excitation to occur, an external source must provide the required energy. In this case, light is used. The following equation is used for the calculation of the energy of such light

Equation 1 Energy of Light

$$E = h * c/\lambda$$

where E is energy, h is Plank's constant, c is the speed of light, and λ is the wavelength of light. This leads to the following relationship

Equation 2 Proportionality of Energy to Wavelength

$$E \alpha 1/\lambda$$

which shows the inverse relationship between energy and wavelength.[46] The absorption energy for an excited molecule is not equivalent to the energy emitted. The emission energy is actually lower since some energy is lost during internal conversion. This loss of energy causes

fluorescence to occur at a longer wavelength since the two are inversely proportional to each other.[41] The resulting excitation and emission spectra would therefore overlap each other. The difference between the maximum of the absorption peak and the maximum of the fluorescence peak is known as the Stokes Shift, and is represented by the following expression

Equation 3 Stokes Shift

$$\Delta\bar{\upsilon} = \bar{\upsilon}_a - \bar{\upsilon}_f$$

where $\Delta\bar{\upsilon}$ is in wavenumbers, and $\bar{\upsilon}_a$ and $\bar{\upsilon}_f$ are the maximum wavelength of the absorption and emission peaks, respectively.[42]

One of the common aspects of fluorescence is that the same emission spectrum is observed regardless of the excitation wavelength. This concept is known as Kasha's rule.[41] When molecules get excited to higher levels of both the electronic and vibrational states, the excess energy is diffused causing the fluorophore to be left in the lowest vibrational level of S_1. The relaxation happens in about 10^{-12} s and is due to an overlap of equal energy states. The relaxation causes the emission spectra to be independent of the excitation wavelength for the vast majority of molecules.[41]

4.2. Results and Discussion

The diamidines selected for this study were chosen to study the effect of structural variation on fluorescence. The fluorescence comparison is done using an excitation slitwidth of 2.5 and an emission slitwidth of 5. These slitwidths parameters were chosen since they provided the greatest amount of comparable data. For the discussion, the compounds are divided into groups based on structural similarity and are all compared to DB 75. Throughout this

dissertation, diamidine structures are shown as a free base; however, when in biological systems, they are protonated and are dications. The compounds used in the fluorescence studies were dihydrochloride salts.

4.2.1. Comparison of Data in Table 2: DB 75, 351, 1213, 1751, 1620, 262, and 320

The first set of compounds for comparison are located in Table 2 and include DB 75, 351, 1213, 1751, 1620, 262, and 320. These compounds have a general structure that consists of amidine-phenyl-heterocycle-phenyl-amidine. The heterocycle moieties include furan (DB 75), thiophene (DB 351), selenophene (DB 1213), tellurophene (DB 1751), thiazole (DB 1620), pyrrole (DB 262) and *N*-methyl pyrrole (DB 320).

These seven compounds provided an excitation wavelength range of 339-376 nm and an emission wavelength range of 433-476 nm. DB 75 has an excitation wavelength of 359 nm and an emission wavelength of 466 nm. Use of a thiophene in DB 351 instead of the furan of DB 75 lowers the excitation wavelength by 3 nm to 356 nm and the emission wavelength by 20 nm to 446 nm. The substitution of a selenophene in DB 1213 for the furan of DB 75 causes an increase in the excitation wavelength by 3 nm to 362 nm and a decrease in the emission wavelength by 16 nm to 450 nm. Comparing the tellurophene of DB 1751 to DB 75 causes a 9 nm increase to 368 nm and a 6 nm decrease to 460 nm for the excitation and emission wavelengths, respectively. The use of pyrrole in DB 262 as compared to the furan of DB 75 results in an increase in both the excitation wavelength by 17 nm to 376 nm and the emission wavelength by 10 nm to 476 nm. When the pyrrole is substituted with a methyl group as in DB 320 and compared to DB 75 the excitation wavelength decreases by 2 nm to 357 nm and the emission wavelength increases by 9 nm to 475 nm. DB 75 yielded the highest emission intensity

Table 2 Comparison of DB 75, 351, 1213, 1751, 1620, 262, and 320

DB #	Excitation λ max (nm)	Emission λ max (nm)	Emission Intensity (au)	Structure
75	359	466	295	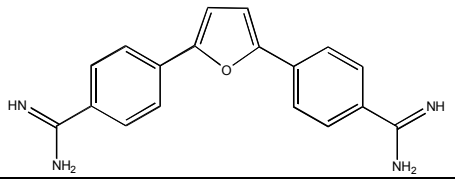
351	356	446	249	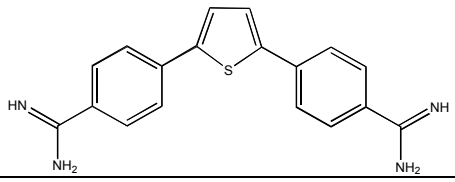
1213	362	450	61	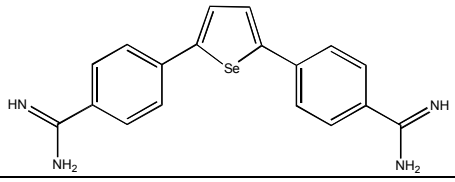
1751	368	460	1	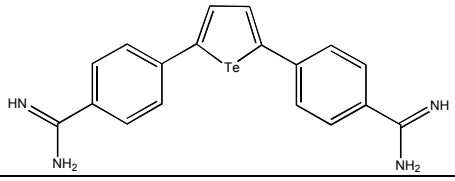
1620	339	433	188	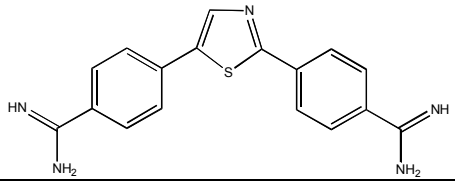
262	376	476	2	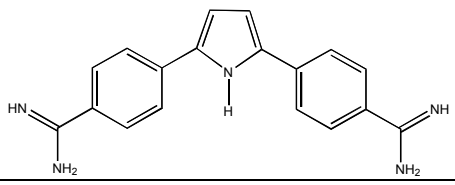
320	357	475	1	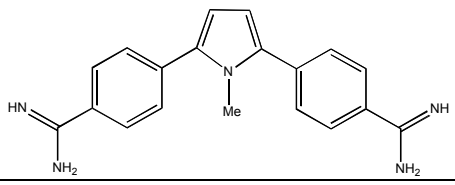

Note: All data is uncorrected and fluorescence measurements were taken at excitation slitwidth of 2.5 and an emission slitwidth of 5. Excitation concentration is 1.66 μM to 16.66 μM and emission concentration is 1 μM.

of 295 au. As compared to DB 75, DB 351 has an emission intensity that was 46 au less at 249 au and DB 1620 has an intensity that was 107 au less at 188 au. The emission intensity of DB 1213 was 234 au less than that of DB 75 at 61 au. The emission intensities of DB 1751, 262, and 320 were barely detectable. As a result, DB 262 was assigned a value of 2 au and both DB 1751and 320 were assigned a value at 1 au

The heteroatoms O (DB 75), S (DB 351), Se (DB 1213), and Te (DB 1751) are in group 6A of the periodic table. For this group of compounds, there is not a significant correlation in the emission and excitation wavelengths. A trend in the data shows that the fluorescence intensity decreases as the atomic radius of the heteroatom increases. This is demonstrated as the emission intensity decreases with the radius increase from O (DB 75) to S (DB 351) to Se (DB 1213) to Te (DB 1751). Nitrogen lies in period 5A of the periodic table and has an atomic radius slightly larger than oxygen. If it followed the trend associated with the heteroatoms of period 6A then one would expect the emission intensity to be comparable to that of DB 75, the O containing heterocyclic molecule. Instead, DB 262 and 320 have emission intensities that are more in line with that of Te (DB 1751), which has a much larger radius. It is suggested that the two compounds with nitrogen containing heterocycles, DB 262 and 320, essentially lack fluorescence, as compared to DB 75, since the processes of photoluminescence that fail to produce radiation are more efficient than those that produce radiation. As a result, it is proposed that DB 262 and 320 undergo intersystem crossing, which would contribute to the inability to detect appreciable emission intensity.[47] DB 1620 has two heteroatoms, sulfur and nitrogen. The thiazole molecule (DB 1620) has an emission intensity that lies between the assigned value of the pyrrole heterocycle (DB 262) and the thiophene heterocycle (DB 351). It is suggested that the presence of nitrogen in the thiazole molecule negatively affects the overall fluorescence since

the emission intensity of DB 1620 is not in line with that of the other sulfur containing molecule (DB 351). The lower emission wavelength exhibited by DB 1620 as compared to DB 351 is expected since an increase in the number of nitrogen atoms in a molecule causes a hypsochromic shift due to the decrease in the π electron conjugation.[48] DB 1620 fluoresces in the violet region of the visible spectrum whereas the other compounds fluoresce in the blue range.

4.2.2. Comparison of Data in Table 3: DB 75, 820, and 829

The second group of compounds for comparison is DB 75, 820, and 829 and the structures are shown in Table 3. Both DB 829 and 820 are derivatives of DB 75, which consists of amidine-phenyl-furan-phenyl-amidine structure. DB 820 has one of the phenyl groups replaced with a pyridyl group and DB 829 has both phenyl groups replaced with pyridyl groups.

Table 3 Comparison of DB 75, 820, and 829

DB #	Excitation λ max (nm)	Emission λ max (nm)	Emission Intensity (au)	Structure
75	359	466	295	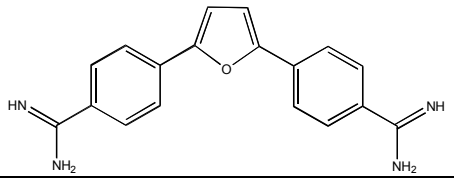
820	364	460	388	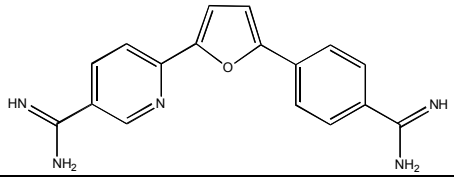
829	362	432	524	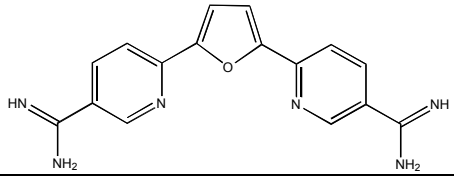

Note: All data is uncorrected and fluorescence measurements were taken at excitation slitwidth of 2.5 and an emission slitwidth of 5. Excitation concentration is 1.66 μM to 16.66 μM and emission concentration is 1 μM.

These three compounds provided an excitation wavelength range of 339-364 nm and an emission wavelength range of 432-466 nm. DB 75 has an excitation wavelength of 359 nm and an emission wavelength of 466 nm. Substitution of one of the phenyl groups in DB 75 for a pyridyl group to form DB 820 increases the excitation wavelength by 5 nm to 364 nm but lowers the emission wavelength by 6 nm to 460 nm, as compared to DB 75. Substitution of both of the phenyl groups in DB 75 for pyridyl groups to form DB 829 increases the excitation wavelength by 3 nm to 362 nm but lowers the emission wavelength by 34 nm to 432 nm, as compared to DB 75. DB 75 has the lowest emission intensity of the three compounds at 295 au. As compared to DB 75, DB 820 has an emission intensity that was 93 au more at 388 au and DB 829 has an intensity that was 229 au more at 524 au.

There is no obvious correlation between the excitation wavelengths for the three compounds but the emission wavelength decreases with each substitution of a pyridyl group for a phenyl group. This is expected since a hypsochromic shift occurs as the number of nitrogen atoms in a molecule increases as a result of the decrease in the π electron conjugation.[48] The emission intensity has an opposing trend since it increases with the subsequent replacement of a CH unit by a nitrogen atom. In addition, DB 75 and 820 emit in the blue region of the visible spectrum while DB 829 emits in the violet region.

4.2.3. Comparison of Data in Table 4: DB 75, 832, and 943

The third set of compounds for analysis includes DB 75, 832, and 943 (Table 4). The structure of DB 75 is amidine-phenyl-furan-phenyl-amidine. DB 832 has a structure of amidine-phenyl-furan-furan-amidine while the structure of DB 943 is amidine-phenyl-phenyl-furan-amidine.

These three compounds provided an excitation wavelength range of 335-368 nm and an emission wavelength range of 427-470 nm. The substitution of furan for a phenyl in DB 75 to yield DB 832 causes a slight increase in the excitation and emission wavelengths by 9 nm to 368 nm and by 4 nm to 470 nm, respectively. Conversely, when the layout of DB 75 is changed from amidine-phenyl-furan-phenyl-amidine to that of amidine-phenyl-phenyl-furan-amidine in DB 943, both wavelengths are lowered. The excitation wavelength decreases by 24 nm to 335 nm and the emission wavelength decreases by 39 nm to 427 nm. DB 75 yielded the highest emission intensity of 295 au. As compared to DB 75, DB 832 has an emission intensity that was 39 au less at 256 au and DB 943 has an intensity that was 93 au less at 202 au. The emission data shows that DB 943 fluoresces in the violet range of the visible spectrum whereas DB 75 and 832 fluoresce in the blue region.

Table 4 Comparison of DB 75, 832, and 943

DB #	Excitation λ max (nm)	Emission λ max (nm)	Emission Intensity (au)	Structure
75	359	466	295	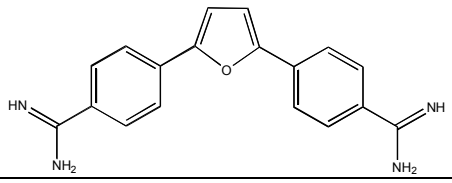
832	368	470	256	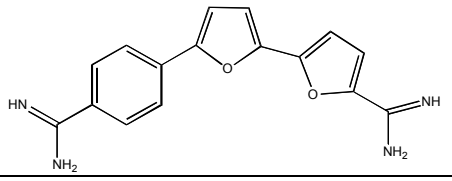
943	335	427	202	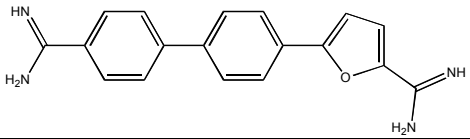

Note: All data is uncorrected and fluorescence measurements were taken at excitation slitwidth of 2.5 and an emission slitwidth of 5. Excitation concentration is 1.66 μM to 16.66 μM and emission concentration is 1 μM.

This data shows that the substitution of a furan in DB 832 for a phenyl group in DB75 lowers the fluorescence intensity while only increasing the corresponding wavelengths slightly. The data also shows that the structural rearrangement of the individual components of DB 75 to yield DB 943 significantly lowers the excitation and emission wavelengths as well as the emission intensity as compared to DB 75. The conjugation within the molecules was maintained so the depression of the emission intensity values were unexpected since it is believed that conjugation enhances fluorescence emission and intensity.[47] Most five membered heterocyclic rings are not considered fluorescent themselves but when coupled with phenyl rings, significant fluorescence is seen.[48] With this in mind, it is believed that the emission intensity of DB 832 is slightly depressed as compared to that of DB 75 since an additional phenyl has been replaced by another furan. The most advantageous position for the location of the non-fluorescent furan is between two phenyl rings.[48] The further decrease in the wavelengths and emission intensity of DB 943 as compared to both DB 75 and 832 may be the result of the torsional twist of the biphenyl unit.

4.2.4. Comparison of Data in Table 5: DB 75, 832, 1347 and 1871

The fourth set of compounds to be analyzed are listed in Table 5 and include DB 75, 832, 1347 and 1871. The structure of DB 75 is amidine-phenyl-furan-phenyl-amidine. DB 832 has a structure of amidine-phenyl-furan-furan-amidine while the structure of DB 1347 is amidine-furan-furan-furan-amidine. The last compound in the group is DB 1871 and it has a structure of amidine-indole-furan-furan-amidine.

This group of compounds provided an excitation wavelength range of 359-380 nm and an emission wavelength range of 466-533 nm. DB 75 has an excitation wavelength of 359 nm and an emission wavelength of 466 nm. The substitution of furan for one phenyl group in DB 75 to

Table 5 Comparison of DB 75, 832, 1347, and 1871,

DB #	Excitation λ max (nm)	Emission λ max (nm)	Emission Intensity (au)	Structure
75	359	466	295	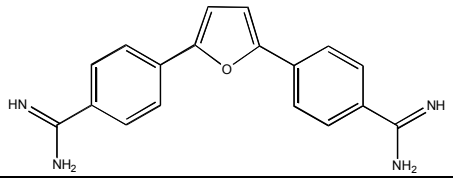
832	368	470	256	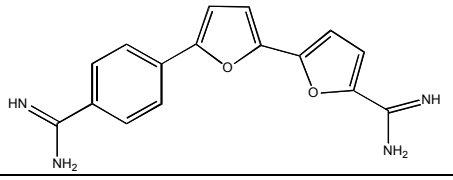
1347	380	470	315	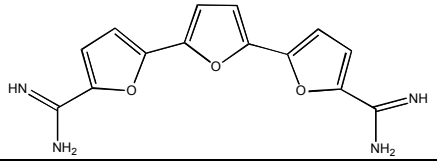
1871	390	533	2	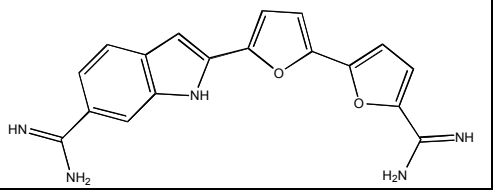

Note: All data is uncorrected and fluorescence measurements were taken at excitation slitwidth of 2.5 and an emission slitwidth of 5. Excitation concentration is 1.66 μM to 16.66 μM and emission concentration is 1 μM.

yield DB 832 causes a increase in the excitation wavelength by 9 nm to 368 nm and an increase in the emission wavelength by 4 nm to 470 nm. When both phenyl groups of DB 75 are converted to furan to yield DB 1347, the excitation and emission wavelengths increase by 21 nm and 4 nm, to 380 nm and 470 nm, respectively. If DB 1871 is compared to DB 75, one phenyl group is replaced with furan and the other is replaced with indole. This change causes an increase in the excitation wavelength by 31 nm to 390 nm and an increase in the emission wavelength by 67 nm to 533 nm. DB 1871 fluoresces in the green region of the visible spectrum while DB 75, 832, and 1347 all fluoresce in the blue region. The emission intensity of DB 75

was 295 au. As compared to DB 75, DB 832 has an emission intensity that was 39 au less at 256 au and DB 1347 has an intensity that was 20 au more at 315 au. DB 1871 had an emission intensity that barely registered and was assigned a value of 2 au.

This data shows that the first phenyl to furan substitution in DB 75 to provide DB 832 does not greatly increase the excitation and emission wavelengths but essentially maintains the emission intensity. As previously stated, five-membered heterocyclic rings are generally not fluorescent on there own and their best location to exhibit fluorescence is between two phenyl groups.[48] With this in mind, it is believed that the emission intensity of DB 832 is slightly depressed as compared to that of DB 75 as a result of there being two furan moieties present instead of just one. A subsequent substitution of replacing the second phenyl group with a second furan to yield DB 1347, a molecule with three furans, increases the excitation wavelength emission intensity more than both DB 75 and DB 832. When the substitution of one phenyl group for indole and the second phenyl for furan in DB 75 to produce DB 1871 occurs, it causes another marginal increase in the excitation wavelength but a significant increase in the emission wavelength. The large emission wavelength may be caused by the larger conjugated indole ring systems since it is known that the coupling of a non-fluorescent five-membered ring with a phenyl group causes an increase in the emission as a result of increased conjugation.[48] However, the emission intensity for DB 1871 is quite low. DB 832 and DB 1871 are structurally similar except for the fact that DB 832 has a phenyl group, which is replaced by an indole in DB 1871. The phenyl to indole substitution causes both the excitation and emission wavelengths to increase. The opposite is true for the emission intensity since the intensity of DB 1871 is barely detectable while DB 832 yields a reading of 256 au.

4.2.5. Comparison of Data in Table 6: DB 75, 921, 1883, and 1871

The fifth set of compounds for analysis includes DB 75, 921, 1883, and 1871 (Table 6). The structure of DB 75 is amidine-phenyl-furan-phenyl-amidine. DB 921 has a structure of amidine-benzimidazole-phenyl-phenyl-amidine while the structure of DB 1883 is amidine-indole-phenyl-phenyl-amidine. The last compound in the group is DB 1871 and it has a structure of amidine-indole-furan-furan-amidine.

This group of compounds provided an excitation wavelength range of 324-390 nm and an emission wavelength range of 0-533 nm. DB 75 has an excitation wavelength of 359 nm and an emission wavelength of 466 nm. DB 921 has a lower excitation wavelength and a slightly higher emission wavelength as compared to DB 75. The excitation wavelength is 35 nm lower at 324 nm and the emission wavelength is 3 nm higher at 472 nm. The excitation wavelength of DB 1883 is 353 nm, which is 6 nm lower than that of DB 75 but it did not show detectable fluorescence under the measured conditions used. DB 1871 has an excitation wavelength that is 31 nm higher than DB 75 at 390 nm and an emission wavelength that is 74 nm higher than that of DB 75 at 533 nm. DB 75 has an emission intensity of 295 au. DB 921 has an emission intensity that is 249 au lower at 46 au and DB 1883 provides no fluorescence at these conditions. The emission intensity of DB 1871 is barely detectable and is assigned a value of 2 au, 293 au less than that of DB 75.

DB 1883 failed to show an emission wavelength under the conditions of measurement.. In comparison of DB 75 to that of DB 921, a phenyl group and the furan are replaced with benzimidazole and a phenyl group. The benzimidazole contains two nitrogen atoms. One of the benzimidazole nitrogen atoms has a lone pair that contributes to the aromaticity of the ring. It is suggested that the nitrogen containing heterocycles exhibit a decreased fluorescence intensity, as

Table 6 Comparison of DB 75, 921, 1883, and 1871

DB #	Excitation λ max (nm)	Emission λ max (nm)	Emission Intensity (au)	Structure
75	359	466	295	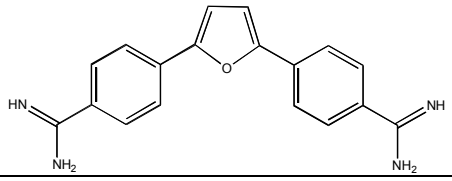
921	324	472	46	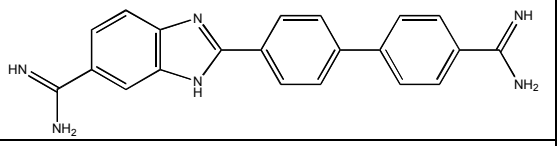
1883	353	N/A	Not detected	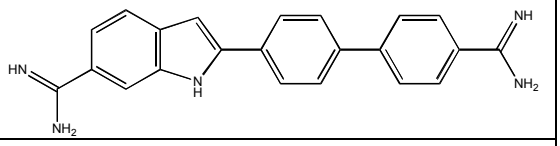
1871	390	533	2	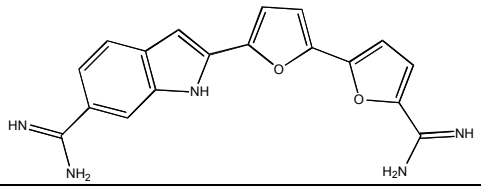

Note: All data is uncorrected and fluorescence measurements were taken at excitation slitwidth of 2.5 and an emission slitwidth of 5. Excitation concentration is 1.66 μM to 16.66 μM and emission concentration is 1 μM.

compared to DB 75, since the processes of photoluminescence that fail to produce radiation are more efficient than those that produce radiation. As a result, it is proposed these compounds undergo intersystem crossing, which would contribute to the detection of lower emission intensities.[47] It should be noted that DB 1871 fluoresces in the green region of the visible spectrum while DB 75 and 921 fluoresce in the blue region.

4.2.6. Comparison of Data in Table 7: DB 75, 262, 320, and 1304

The sixth set of compounds for analysis includes DB 75, 262, 320, and 1304. These compounds are shown in Table 7 and have a general structure that consists of amidine-phenyl-5-

membered ring-phenyl-amidine. The heterocycle moieties include furan (DB 75), pyrrole (DB 262), *N*-methyl pyrrole (DB 320), and *N*-ethyl pyrrole (DB 1304).

Table 7 Comparison of DB 75, 262, 320, and 1304

DB #	Excitation λ max (nm)	Emission λ max (nm)	Emission Intensity (au)	Structure
75	359	466	295	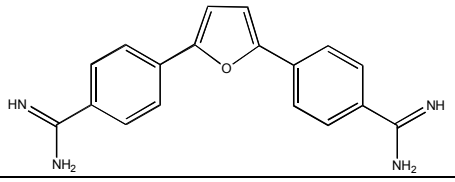
262	376	476	2	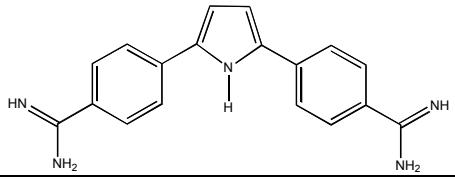
320	357	475	1	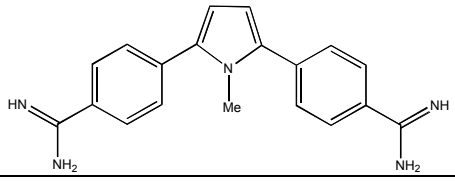
1304	345	N/A	Not detected	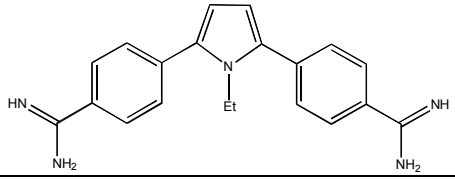

Note: All data is uncorrected and fluorescence measurements were taken at excitation slitwidth of 2.5 and an emission slitwidth of 5. Excitation concentration is 1.66 μM to 16.66 μM and emission concentration is 1 μM.

This group of compounds provided an excitation wavelength range of 313-376 nm and an emission wavelength range of 345-476 nm. DB 75 has an excitation wavelength of 359 nm and an emission wavelength of 466 nm. DB 262 has higher excitation and emission wavelengths as compared to DB 75. The excitation wavelength is 17 nm higher at 376 nm and the emission wavelength is about 10 nm higher at 476 nm. The excitation wavelength of DB 320 is lower

than that of DB 75 by 2 nm at 357 nm but the emission wavelength is higher by about 9 nm at 475 nm. DB 1304 has an excitation wavelength that is 14 nm lower than that of DB 75 at 345 nm but it failed to provide detectable emission under these conditions. As stated before, DB 1304 failed to provide an emission signal or intensity reading. DB 262 and 320 gave quite low emission intensities. DB 262 was assigned readings of 2 au and DB 320 was assigned a reading of 1 au.

The excitation and emission wavelengths were very similar for the compounds compared in Table 7. A significant observation is that when the oxygen of DB 75 is replaced with an NH in DB 262 or a N-methyl in DB 320, the emission intensity plummets so that it is barely detectable. The use of pyrrole greatly reduces the emission intensity and is consistent with numerous observations for N-heterocycles in the literature.[47]

4.2.7. Comparison of Data in Table 8: DB 75, 914, 1692, 1464, and 1680

The seventh set of compounds are analyzed in Table 8 and include DB 75, 914, 1692, 1464, and 1680. The structure of DB 75 is amidine-phenyl-furan-phenyl-amidine. DB 914 has a structure that is amidine-phenyl-furan-furan phenyl-amidine whereas DB 1692 has a structure of amidine-phenyl-furan-furan-furan-amidine. DB 1464 has a structure that consists of a series of four furan moieties flanked by an amidine on each side and DB 1680 is a series of five furan moieties flanked by an amidine on each side.

This group of compounds provided an excitation wavelength range of 359-419 nm and an emission wavelength range of 466-549 nm. DB 75 has an excitation wavelength of 359 nm and an emission wavelength of 466 nm. DB 914 has higher excitation and emission wavelengths as compared to DB 75. The excitation wavelength is 33 nm higher at 392 nm and the emission

wavelength is 82 nm higher at 549 nm. DB 1692 has an excitation wavelength that is 400 nm and an emission wavelength that is 546 nm, which is 41 nm and 80 nm higher, respectively, as

Table 8 Comparison of DB 75, 914, 1692, 1464, 1680, and 1315

DB #	Excitation λ max (nm)	Emission λ max (nm)	Emission Intensity (au)	Structure
75	359	466	295	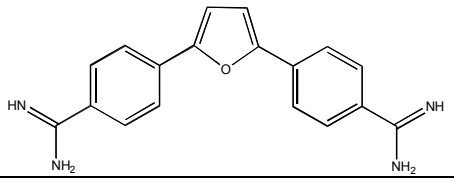
914	392	549	10	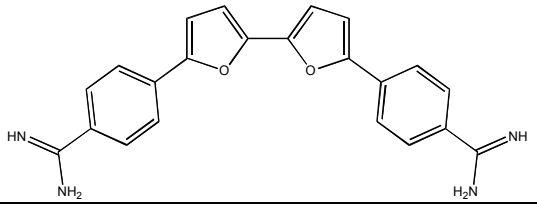
1692	400	546	9	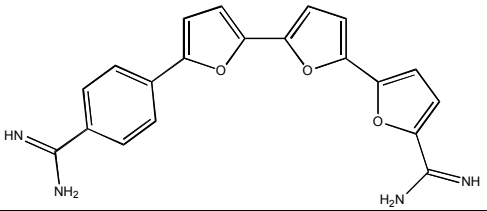
1464	405	544	7	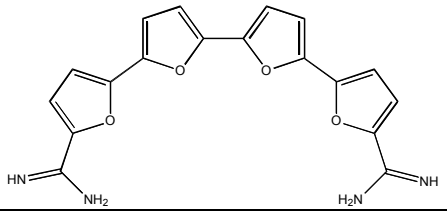
1680	419	538	2	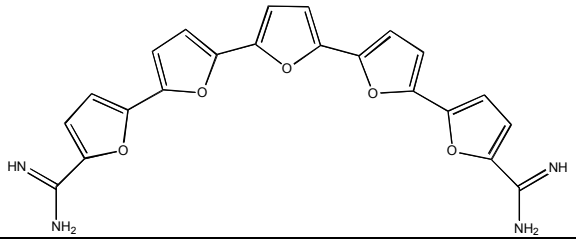

Note: All data is uncorrected and fluorescence measurements were taken at excitation slitwidth of 2.5 and an emission slitwidth of 5. Excitation concentration is 1.66 μM to 16.66 μM and emission concentration is 1 μM.

compared to that of DB 75. DB 1464 also has elevated excitation and emission wavelengths. The excitation wavelength is 45 nm higher at 405 nm and the emission wavelength is 78 nm higher at 544 nm, as compared to DB 75. The excitation wavelength of DB 1680 is 60 nm higher and the emission wavelength is 62 nm higher than that of DB 75 at 419 nm and 538 nm, respectively. DB 75 had the highest emission intensity at 295 au and the readings for the remainder of the compounds in the series were highly depressed. DB 914 has an emission intensity of 10 au while that of DB 1692 was 1 au lower at 9 au. DB 1464 has an emission intensity of 7 au and DB 1680 emission intensity was assigned a value of 2 au.

The data shows that lengthening the molecule with the addition of furan and phenyl moieties generally results in longer excitation wavelengths under these conditions and all were greater than that of DB 75. The compounds also have increased emission wavelengths as compared to DB 75 so the same effect with regards to lengthening the molecule holds true for the emission wavelength as well. It is believed that this bathochromic shift that occurs in the emission wavelength is the result of greater extended conjugation, i.e. 18 electrons in DB 75 versus 24 in the others.[49] The same cannot be said for the emission intensity. If the compounds that did fluoresce are compared to that of DB 75, it can be seen that the emission intensities were all drastically reduced. It is believed that the depressed intensity values are a result of torsion angle rotation due to repulsive van der Waals interactions, which disrupts the planarity that is required for optimal fluorescence.

4.2.8. Comparison of Data in Table 9: DB 75 and 569

The eighth group of compounds for comparison consists of DB 75 and DB 569 and they are compared in Table 9. The structure of DB 75 is amidine-phenyl-furan-phenyl-amidine and DB 569 is a *N*-phenyl amidine derivative of DB 75.

DB 75 has an excitation wavelength of 359 nm and an emission wavelength of 466 nm while DB 569 has essentially the same excitation wavelength at 358 nm but has an emission wavelength that is 20 nm lower at 446 nm. The emission intensity of DB 75 is 295 au but DB 569 has a considerably lower intensity at 6 au.

Table 9 Comparison of DB 75 and 569

DB #	Excitation λ max (nm)	Emission λ max (nm)	Emission Intensity (au)	Structure
75	359	466	295	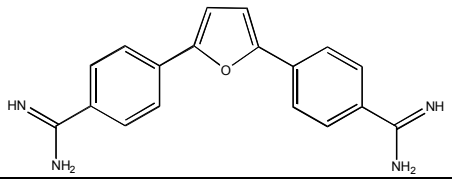
569	358	446	6	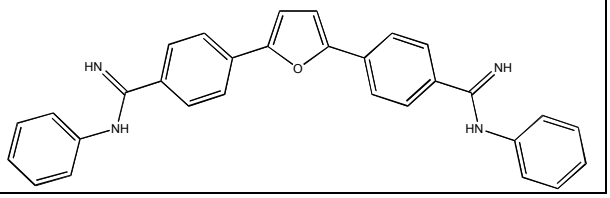

Note: All data is uncorrected and fluorescence measurements were taken at excitation slitwidth of 2.5 and an emission slitwidth of 5. Excitation concentration is 1.66 μM to 16.66 μM and emission concentration is 1 μM.

The substitution of hydrogen in the NH_2 portion of the amidine for a phenyl group does not affect the excitation wavelength, as compared to DB 75. However, the change does lower the emission wavelength and drastically reduces the emission intensity. The substitution of the phenyl group for hydrogen potentially lengthens the conjugation of the molecule so it is expected that the emission wavelength would be higher for DB 569 as compared to DB 75. This does not occur so one possible explanation is that the substitution causes a conformational change in DB 569 that makes the molecule non-planar, thereby reducing the fluorescence wavelength and emission intensity below the values shown in DB 75. Both compounds fluoresce in the blue region of the visible spectrum.

4.2.9. Comparison of Data in Table 10: DB 75, 613, 667, and 766

The last group of compounds for comparison includes DB 75, 613, 667, and 766 (Table 10). DB 75 is an amidine and the other three compounds are called reversed amidines. DB 75 has the structure of amidine-phenyl-furan-phenyl-amidine. DB 613 has the structure of phenyl-reversed amidine-phenyl-furan-phenyl-reversed amidine-phenyl. DB 667 and 766 are derivatives of DB 613. In DB 667, the terminal phenyl groups have been replaced with pyridyl

Table 10 Comparison of DB 75, 613, 667, and 766

DB #	Excitation λ max (nm)	Emission λ max (nm)	Emission Intensity (au)	Structure
75	359	466	295	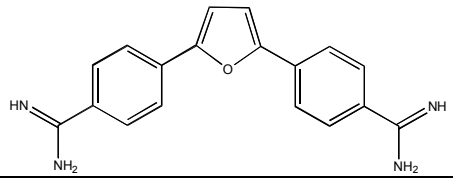
613	343	N/A	Not detected	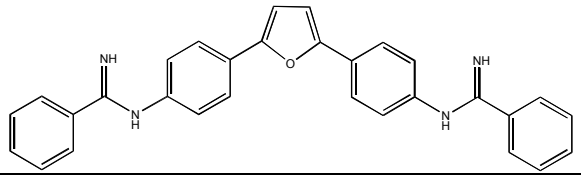
667	347	N/A	Not detected	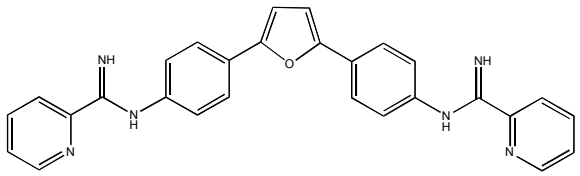
766	361	N/A	Not detected	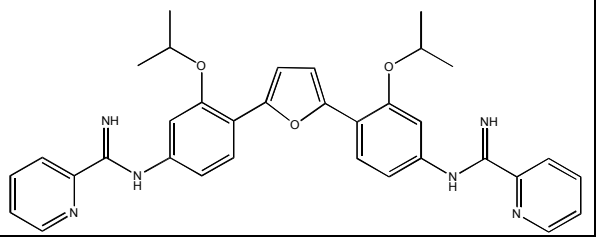

Note: All data is uncorrected and fluorescence measurements were taken at excitation slitwidth of 2.5 and an emission slitwidth of 5. Excitation concentration is 1.66 μM to 16.66 μM and emission concentration is 1 μM.

groups and DB 766 retains the terminal pyridyl groups as in DB 667 but has an additional substitution of a 2-isopropoxy group on the phenyl groups.

This group of compounds provides an excitation wavelength range of 343-361 nm and an emission wavelength up 466 nm. DB 75 has an excitation wavelength of 359 nm and an emission wavelength of 466 nm. The excitation wavelengths for DB 613 and 667 are reduced by 16 nm and 12 nm as compared to DB 75, to yield values of 343 nm and 347 nm, respectively. DB 766 has an excitation wavelength that is higher than that of DB 75 by 2 nm at 361 nm. Unfortunately, none of the reversed amidines gave detectable fluoresce under these conditions.

The conversion of the amidine to the reversed amidine eliminates fluorescence under these conditions, which is thought to be due, in part, to the disruption of the elongated conjugated system.

4.3. Conclusions

Unifying correlations between structure and the corresponding emission intensity are difficult to recognize, however some trends were seen for the excitation and emission wavelengths. These occurrences include the following:

- As you go down the period of the periodic table, the atomic radii of the atoms increases but the corresponding emission intensity of the heterocyclic containing 5-membered ring decreases;
- Compounds with nitrogen containing heterocycles may exhibit decreased or a lack of detectable emission intensity measurements due to the importance of processes that fail to produce radiation, i.e. intersystem crossing, being more energy efficient that fluorescence;

- Generally, 5-membered heterocyclic rings are not known to independently fluoresce but if the 5-membered heterocycle ring is conjugated to other aromatic or heteroaromatic systems fluorescence can be observed;
- Generally, *N*- heterocycles do not exhibit significant fluorescence due to a propensity for intersystem crossing in the excited state;
- Extending the conjugation of a molecule generally causes an increase in the emission wavelength;
- The larger the molecule and the more bonds that have the possibility of free rotation, the more likely the molecule will twist into a non-planar state due to repulsive van der Waal interactions, which will reduce fluorescence emissions;
- Substitution of a phenyl group for an amidine hydrogen or with pyridyl (reversed amidines) potentially increases conjugation but causes the molecule to be less planar, thereby leading to a decreased emission wavelength and intensity.

4.4. Experimental

The excitation wavelengths were measured using a Cary 300 Bio UV-Visible spectrometer and the emission wavelengths and corresponding intensities were measured using the Cary Eclipse Fluorescence Spectrometer.

A 1mM stock solution of the DB compounds in H_2O were prepared and stored in a refrigerator when not in use. To determine the excitation wavelength, the stock solution was added to 3 mL of H_2O in increments of 5 μL with the upper limit of stock solution being 50 μL (concentration = 1.66 μM to 16.66 μM) and scanned from 280 to 800 nm. To determine the emission wavelength, 3 μL of the stock solution was added to 3 mL of MES buffer (concentration = 1 μM) and scanned at varying slitwidths. All measurements were taken at room

temperature and the slitwidths used in the previous tables were an excitation slitwidth of 2.5 and an emission slitwidth of 5. These slitwidths parameters were chosen since they provided the greatest amount of comparable data. The wavelengths are accurate to +/- 2 nm and the intensity measurements result from a flat detection response across the wavelength range. Error in emission intensity is 5%.

5. Appendix

5.1. Appendix A: Sample Excitation Maximum Curve

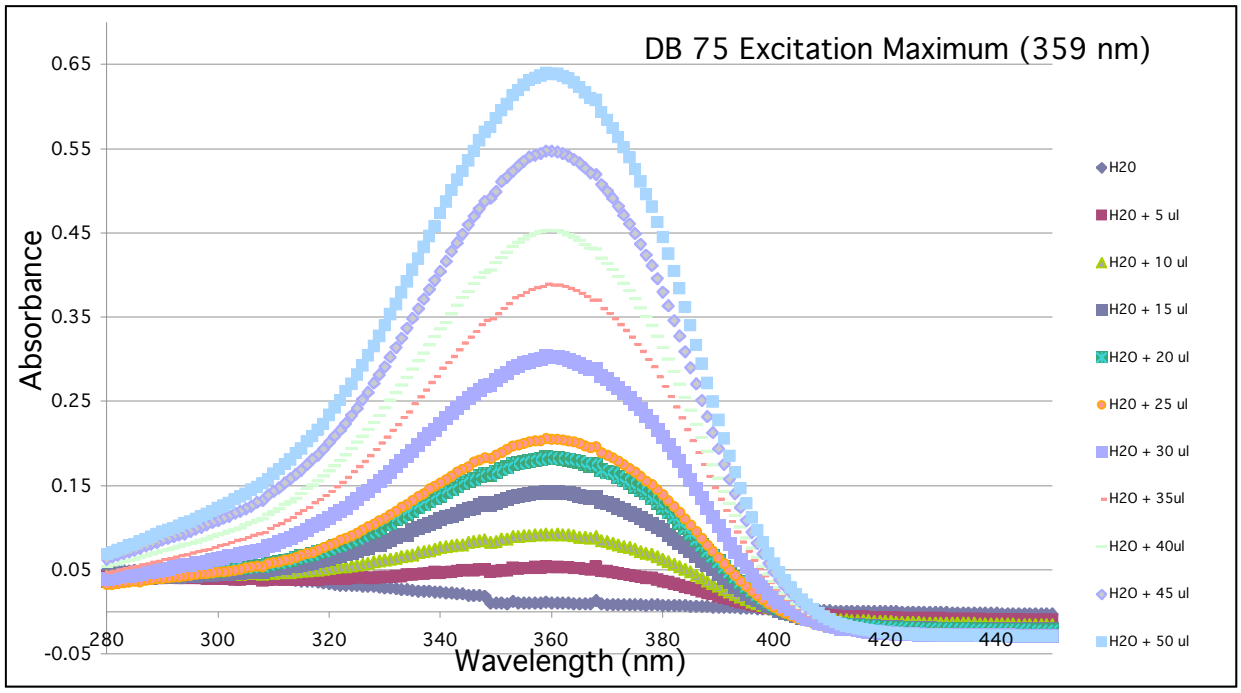

5.2. Appendix B: Sample Spectra

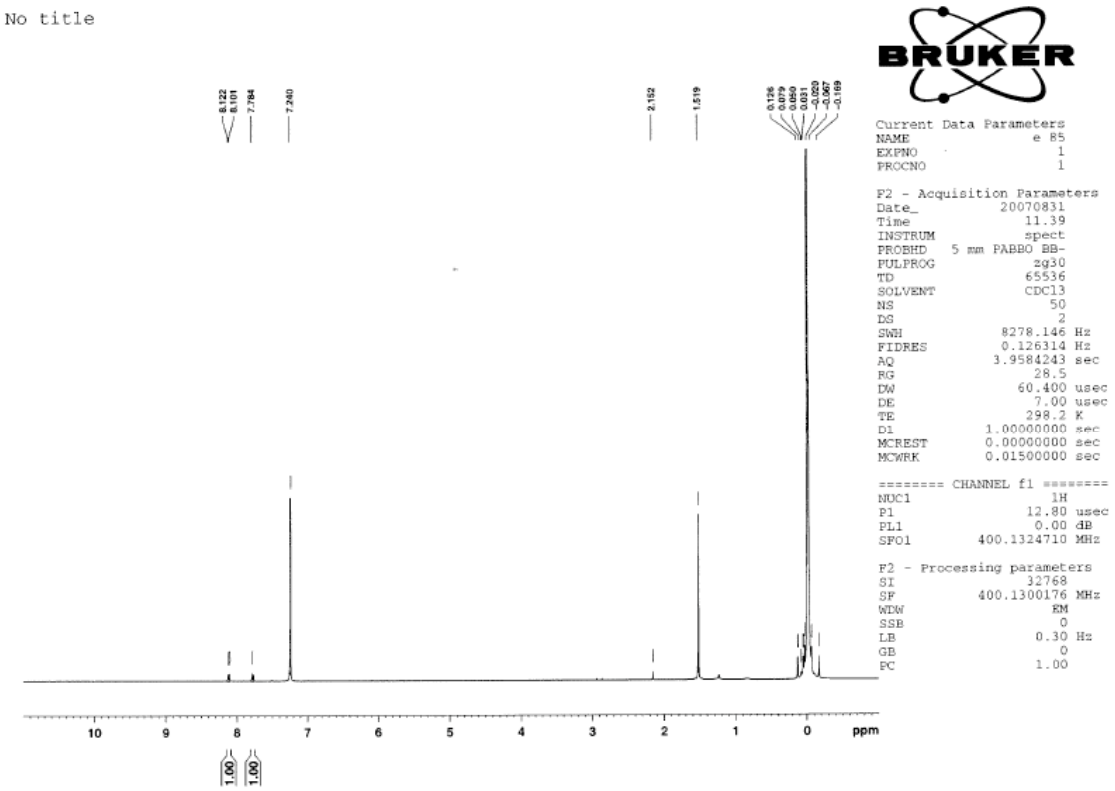

No title

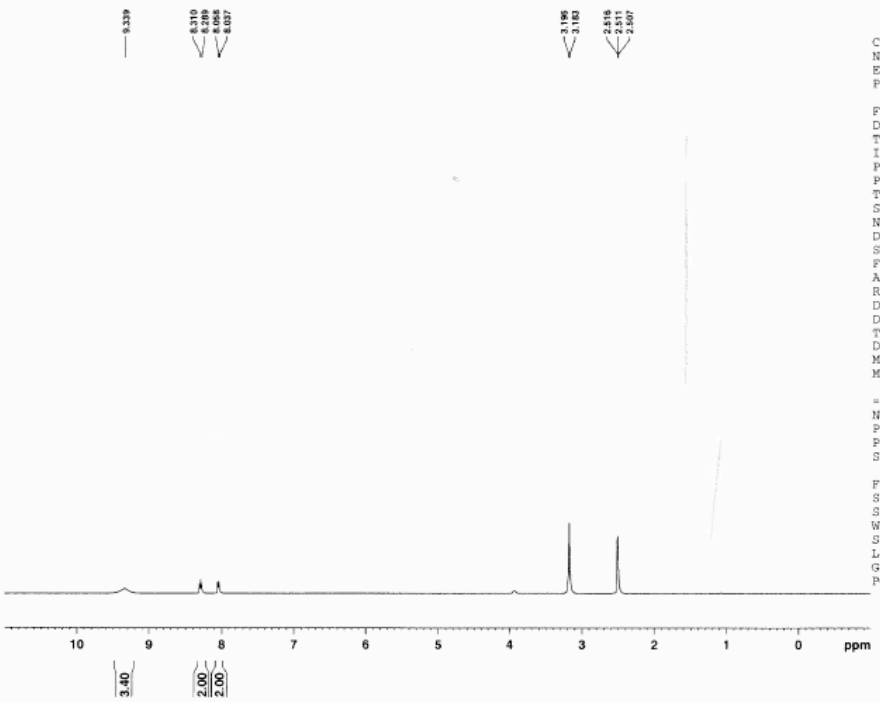

Current Data Parameters
NAME e 96
EXPNO 1
PROCNO 1

F2 - Acquisition Parameters
Date_ 20090306
Time 15.21
INSTRUM spect
PROBHD 5 mm PABBO BB-
PULPROG zg30
TD 65536
SOLVENT DMSO
NS 151
DS 2
SWH 8278.146 Hz
FIDRES 0.126314 Hz
AQ 3.9584243 sec
RG 28.5
DW 60.400 usec
DE 7.00 usec
TE 328.2 K
D1 1.00000000 sec
MCREST 0.00000000 sec
MCWRK 0.01500000 sec

======== CHANNEL f1 ========
NUC1 1H
P1 12.80 usec
PL1 0.00 dB
SFO1 400.1324710 MHz

F2 - Processing parameters
SI 32768
SF 400.1300000 MHz
WDW EM
SSB 0
LB 0.30 Hz
GB 0
PC 1.00

REFERENCES

1. Despommier, D.D., Gwadz, Robert W., Hotez, Peter J., *Parasitic Diseases*. Third ed. 1995: Springer-Verlag.
2. Soeiro, M.N.C., et al., *Aromatic Diamidines as Antiparasitic Agents.* Expert Opinion Investig. Drugs, 2005. **14**(8): p. 957-972.
3. Boutielle, B.O., Odile; Bisser, Sylvie; Dumas, Michel, *Treatment Perspectives for Human African Trypanosomiasis.* Fundamental and Clinical Pharmacology, 2003. **17**: p. 171-181.
4. de Atouguia, J.L.M., Kennedy, Peter G. E., *Neurological aspects of human African trypanosomiasis*, in *Infectious Diseases of the Nervous System*, L.E. Davis, Kennedy, Peter G. E., Editor. 2000, Butterworth Heinemann.
5. Meshnick, S., *The Chemotherapy of African Trypanosomiasis*, in *Parasitic Diseases Vol.2: The Chemotherapy*, J.M. Mansfield, Editor. 1984, Marcel Dekker: New York. p. 165-199.
6. Ganesh, V.M., Suresh Kumar; Smith, Scott A.; Kotwal, Girish J.; Murthy, Krishna H.M., *Structural Basis for Antagonism by Suramin of Heparin Binding to Vaccinia Complement Protein.* Biochemistry, 2005(44): p. 10757-10765.
7. Cunningham, M.L.Z., Marketa J. J. M.; Fairlamb, Alan H., *Mechanism of Inhibition by Trypanothione Reductase and Glutathione Reductase by Trivalent Organic Arsenicals.* European Journal of Biochemistry, 1994(221): p. 285-295.
8. De Koning, H.P.J., Simon, *Adenosine Transporters in Bloodstream Forms of Trypanosoma brucei brucei : Substrate Recognition Motifs and Affinity for Trypanocidal Drugs.* Molecular Pharmacology, 1999(56): p. 1162-1170.
9. Happersberger, H.P.S., Janet; Cowgill, Cynthia; Glocker, Michael O., *Characterization of the Folding Pathway of Recombinant Human Macrophage-Colony Stimulating-Factor β (rhM-CSF β) by Bis-Cysteinyl Modification and Mass Spectrometry.* Proteins: Structure, Function, and Genetics Suppl., 1998(2): p. 50-62.
10. Trumpler, S.N., Sascha; Meermann, Bjorn; Wiesmuller, Gerhard A.; Buscher, Wolfgang; Sperling, Michael; Karst, Uwe, *Detoxification of Mercury Species-An In Vitro Study with Antidotes in Human Whole Blood.* Analytical Bioannalytical Chemistry, 2009(395): p. 1929-1935.
11. Boykin, D.W., *Antimicrobial Activity of the DNA Minor Groove Binders Furamidine and Analogs.* Journal of The Brazilian Chemical Society, 2002. **13**(6): p. 763-771.
12. Finkelstein, R., *Protection of Chick Embryos Against Newcastle Disease Virus By Trypan Blue and Other Compounds.* Journal of Immunology, 1961(87): p. 707-713.
13. Croft, S.L.B., Michael P.; Urbina, Julia A., *Chemotherapy of Trypanosomiasis and Leishmaniasis.* Trends in Parasitology, 2005. **21**(11): p. 508-512.
14. Kierszenbaum, F., *The Chemotherapy of Trypanosoma cruzi Infections (Chagas' Disease)*, in *Parasitic Diseases Vol. 2: The Chemotherapy*, J.M. Mansfield, Editor. 1984, Marcel Dekker Inc.: New York. p. 133-163.
15. Dardonville, C.B., Reto, *Bisguanidine, Bis(2-aminoimidazoline) and Polyamine Derivatives as Potent and Selective Chemotherapeutic Agents Against Trypanosoma brucei rhodesiense. Synthesis and in Vitro Evaluation.* Journal of Medicinal Chemistry, 2004(47): p. 2296-2307.

16. Nunn, C.J., Terence; Neidle, Stephen, *Crystal Structure of d(CGCGAATTCGCG) Complexed with Propamidine, a Short Chain Homologue of the Drug Pentamidine.* Biochemistry, 1993(32): p. 13838-13843.
17. Lansiaux, A., et al., *Distribution of Furamidine Analogs in Tumor Cells: Targeting of the Nucleus or Mitochondria Depending on the Amidine Substitution.* Cancer Research, 2002. **62**: p. 7219-7229.
18. Trent, J.O.C., George R.; Kumar, Arvind; Wilson, W. David; Boykin, David W.; Hall, James Edwin; Tidwell, Richard R; Blagburn, Byron L.; Neidle, Stephen, *Targeting the Minor Groove of DNA: Crystal structures of Two Complexes between Furan Derivatives of Berenil and the DNA Dodecamer d(CGCGAATTCGCG)$_2$.* Journal of Medicinal Chemistry, 1996(39): p. 4554-4562.
19. *Merriam-Webster Online*, F.C. Mish, Editor. 2010.
20. Silverman, R.B., *The Organic Chemistry of Drug Design and Drug Action*. Second ed. 2004: Elsevier Academic Press.
21. Patrick, G.L., *An Introduction to Medicinal Chemistry*. Second ed. 2001: Oxford University Press.
22. Garrett, R.H., Grisham, Charles M., *Biochemistry*. Second ed. 1999: Harcourt College Publishers.
23. Blackburn, G.M.G., Michael J.; Laokes, David; Williams, David M., ed. *Nucleic Acids in Chemistry and Biology*. Third ed. 2006, RSCPublishing.
24. Branden, C.T., John, *Introduction to Protein Structure*. Second ed. 1999: Garland Publishing.
25. Haider, S.P., Gary N.; Read, Martin A.; Neidle, Stephen, *Design and Analysis of G4 Recognition Compounds*, in *DNA and RNA Binders: From Small Molecules to Drugs*, M.B. Demeunynck, C.; Wilson, W. D., Editor. 2003, Wiley. p. 337-359.
26. Franceschin, M., *G-Quadruples DNA Structures and Organic Chemistry: More Than One Connection.* European Journal of Organic Chemistry, 2009: p. 2225-2238.
27. Burge, S.P., Gary N.; Hazel, Pascale; Todd, Alan K.; Neidle, Stephen, *Quadruplex DNA: sequence, topology, and structure.* Nucleic Acids Research, 2006. **34**(19): p. 5402-5415.
28. Organization, W.H., *Human African Trypanosomiasis*. 2009.
29. Wilson, W.D., et al., *Dications That Target the DNA Minor Groove: Compound Design and Preparation, DNA Interactions, Cellular Distribution and Biological Activity.* Curr. Med. Chem. - Anti-Cancer Agents, 2005. **5**(4): p. 389-408.
30. Miao, Y., et al., *Out-of-Shape DNA Minor Groove Binders: Induced Fit Interactions of Heterocyclic Dications with the DNA Minor Groove.* Biochemistry, 2005. **44**: p. 14701-14708.
31. Johnson, J.R. and R. Ketcham, *Thiazolothiazoles. I. The Reaction of Aromatic Aldehydes with Dithiooxamide.* Journal of the American Chemical Society, 1960. **82**: p. 2719-24.
32. Johnson, J.R., D.H. Rotenberg, and R. Ketcham, *Thiazolothiazoles. II. The Parent Heterocycle and Its Carboxylic and Amino Derivatives.* Journal of the American Chemical Society, 1970. **92**: p. 4046.
33. Thomas, D.A., *Derivatives of Thiazolo[5,4-d]thiazole.* Journal of Heterocyclic Chemistry, 1970. **7**(2): p. 457-62.
34. Al-Dujaili, A.H., A.T. Atto, and A.M. Al-Kurde, *Synthesis and Liquid Crystalline Properties of Models and Polymers Containing Thiazolo[5,4-d]thiazole and Siloxane Flexible Spacers.* European Polymer Journal, 2001. **37**: p. 927-932.

35. Ando, S., et al., *Synthesis, Physical Properties and Field-effect Transistors of Novel Thiazolothiazole-phenylene Co-oligomers.* Journal of Materials Chemistry, 2007. **17**(6): p. 553-558.
36. Boere, R.O., R; Reed, R, *Preparation of N,N,N'-tris(trimethylsilyl)amidines; a Convenient Route to Unsubstituted Amidines.* Journal of Organometalic Chemistry, 1987. **331**: p. 161-167.
37. Ismail, M.A., et al., *Dicationic Near-linear Biphenyl Benimidazole Derivatives as DNA-targeted Antiprotozoal Agents.* Bioorganic and Medicinal Chemistry, 2005. **13**: p. 6718-6726.
38. Ismail, M.A.A., Reem K.; Brun, Reto; Wenzler, Tanja; Miao, Yi; Wilson, W.David; Generaux, Claudia; Bridges, Arlene; Hall, James E.; Boykin, David W., *Synthesis, DNA affinity, and Antiprotozoal Activity of Linear Dications: Terphenyl Diamidines and Analogues.* Journal of Medicinal Chemistry, 2006. **49**: p. 5324-5332.
39. Munde, M.I., Mohamed A.; Arafa, Reem; Peixoto, Paul; Collar, Catharine; Liu, Yang; Hu, Laixing; David-Cordonnier, Marie-Helene; Lansiaux, Amelie; Bailly, Christian; Boykin, David W.; Wilson, W. David, *Design of DNA Minor Groove Binding Diamidines That Recognize GC Base Pair Sequences: A Dimeric-Hinge Interaction Motif.* Journal of the American Chemical Society, 2007. **129**: p. 13732-13743.
40. Musetti, C.K., Arvind; Ismail, Mohamed A.; Say, Martial; Barber, Jennifer C. Brown; Lucatello, Lorena; Casatti, Margherita; Munde, Manoj; Sissi, Claudia; Palumbo, Manlio; Boykin, David W.; Wilson, W. David, *SHAPE BASED RECOGNITION AND BINDING TO QUADRUPLEX DNA BY HETEROCYCLIC CATIONS.* In Preparation.
41. Lakowicz, J.R., *Principles of Fluorescence Spectroscopy*. Third ed. 2006: Springer.
42. Valeur, B., *Molecular Fluorescence: Principles and Applications*. 2002, Weinheim: Wiley-VCH.
43. Klessinger, M.M., Josef, *Excited States and Photochemistry of Organic Molecules*. 1995, New York, New York: VCH Publishers.
44. Advanced Imaging Laboratory, D.O.B., University of Victoria, *Epi-fluorescence with the Microscope*. 2005: Victoria, British Columbia, Canada.
45. Baczynski, A.R., Danuta, *Electronic Spectra of Dye Solutions. I. The Mirror Image Rule.* Journal of Fluorescence, 1992. **2**(3): p. 175.
46. Ebbing, D.D., *General Chemistry*. Fifth ed. 1996: Houghton Mifflin Company.
47. Wehry, E.L., *Structural and Environmental Factors in Fluorescence*, in *Fluorescence: Theory, Instrumentation, and Practice*, G.G. Guilbault, Editor. 1967, Marcel Dekker, Inc.: New York, New York. p. 37-132.
48. Berlman, I., *Handbook of Fluorescence Spectra of Aromatic Molecules*. 2nd ed. 1971, New York: Academic Press.
49. Berlman, I., *On an Empirical Correlation between Nuclear Conformation and Certain Fluorescence and Absorption Characteristics of Aromatic Compounds.* Journal of Physical Chemistry, 1970. **74**(16): p. 3085-93.